A Maxwell-Elasto-Brittle rheology for sea ice modelling

Véronique Dansereau, Jérôme Weiss, Pierre Saramito and Philippe Lattes

Answers to reviewer 1

GENERAL COMMENTS

The literature discussion in the introduction is very much focused on sea ice modeling. Damage mechanics has been a vital topic within the glacier and ice sheet modeling community in recent years though, and – even though length, time and stress scales may differ by several orders of magnitude – the models used in this context are conceptually not fundamentally different from those used for sea ice. Particularly, the pioneering work by Pralong et al. (2006) (and several other articles by the same authors) might be important; but also later contributions, such as Duddu and Waisman (2013), could potentially be relevant.

The introduction is indeed focussed on sea ice modelling. However, as the Maxwell-EB model is developed to this specific purpose, we believe this focus is relevant. In particular, discussing the current state of sea ice models in terms of their capability to reproduce sea ice deformation appears essentials. The need for an improved representation of deformation has been discussed extensively in late years: we think it is important to recall this point. As we suggest a *new* mechanical framework for these models, we believe it is also important to state the motivations for our approach, and the fact that we were inspired by the known similarities between the brittle mechanical behaviour of sea ice and the Earth crust, hence by some of the methods used for modelling faults.

Viscoelastic models are indeed used for glacier ice. However, fundamental differences (at least 4) between the present viscoelastic model for sea ice (as well as models for the Earth crust) and viscoelastic models for (polycrystalline) ice and glaciers exist. You are right when stating that time scales, in particular, are key here. Differences in time scales translate into intrinsic differences in the nature of the deformation of sea ice versus of glacier ice: sea ice deforms "rapidly" under the action of the wind and ocean drags, in the *brittle* regime, while glaciers deforms slowly, through viscoplastic deformation of bulk ice.

In the case of viscoelastic models for sea ice and the Earth crust, *instantaneous* elastic deformations are *not* neglected and the viscosity associated with the relaxation of the stress is *not* the dynamical viscosity associated with "true" creep, but rather an *apparent* viscosity, intended to represent the large deformations within the fractured ice cover or faults. This last point is perhaps the most important difference between sea ice- and glacier-type models and in order for the reader to understand the need for an *apparent* rather than the *true* viscosity to model the deformation of sea ice, we believe the comparison to models of the Earth crust is relevant. Finally, the damage criterion in the present and previous (eg., EB) sea ice model is a function of a critical *stress*. In models for glacier flows, damage is often a function of a given cumulative *deformation* threshold and it impacts the viscous flow through the concept of effective stress on Glen's law.

However, we agree that these relevant distinctions deserves a few words and hence we included a short discussion of viscoelastic, damage-based glacier models and their references in the Background (former Introduction) section. To keep this section reasonably short, we somewhat shortened the discussion of models of lithospheric faulting (lines 13-18, page 8).

Damage framework In the damage mechanics literature, a number of different damage measures have been proposed. They differ in how they are included in the constitutive framework and in their level of anisotropy. The damage evolution has to be prescribed depending on the choice of the damage measure. I think the authors should explain their choice in more detail! Why does d_{crit}, and thus the stress, enter the damage evolution equation linearly? The level of anisotropy present in a damage theory is reflected by the tensorial structure of the damage measure. In this light, using a scalar damage measure in a framework which is supposed to model induced anisotropy should carefully be justified. Furthermore, damage healing is known to be delicate with respect to the entropy principle (see also Pralong's article cited above). I am not sure to which extent this issue affects the healing parameterization given in this work, but at least I think it should be addressed as a possible problem.

Different approaches have indeed been used for the damage mechanism. In absence of physical evidences for higher levels of complexity, in developing the Maxwell-EB model we sought the simplest possible formulation and based our approach on isotropic, progressive damage models involving a scalar level of damage variable (e.g., *Amitrano, 1999*, and the EB sea ice model of Girard et al., *2011*). In these models, the decrement in damage enters the damage formulation "linearly". The

main difference in the Maxwell-EB framework is that this decrement in damage, called d_{crit}, is not an *arbitrary constant* as in these previous progressive damage frameworks, which are based on a sub-iteration loop in which damage is allowed to evolve and stress to be redistributed from over to sub-critical elements until a steady-state is reached (i.e., until all states of stress lie within the yield envelope) before the model is incremented and loading resumes. In the present model, damage evolves in "real" model time. Hence if d_{crit} was set constant, the stress drop associated with damaging can be such that stresses will still lie outside of the yield envelope after one model time step. As overcritical stresses are not physical, here we make the logical assumption that the decrement of damage d_{crit} associated with a local damage event should be such that the value of the stress be at most equal to the local critical value.

Concerning anisotropy, we thank the referee for this important point, which was not detailed enough in the initial version of the manuscript. The key point is that, in the present model, an anisotropic damage formulation is not required to generate anisotropy of stress and strain fields. Indeed, in an elastic medium submitted to a non-perfectly isotropic loading (i.e., non-perfectly isotropic with respect to the domain geometry or the heterogeneity present in the material), the elastic kernel associated with a damaged "inclusion" (*Eshelby, 1957*) is anisotropic, hence is the redistribution of stresses. Therefore, the combination of (1) small-scale disorder, (2) damage mechanics in an elastic medium, and (3) this anisotropy of the elastic kernel itself is sufficient to generate anisotropy up to *very large* space scales through successive elastic interactions between damaged elements. We now discuss this point in more details in the *Results* section and add a figure (6) that shows the anisotropic perturbation in the (Coulomb) stress field (σ_1 - qσ_2) generated when uniaxial compression is applied to a uniform rectangular plate with an isotropic, circular inclusion and, similarly, when disorder is introduced in the model at the element scale.

Finally, concerning the entropy principle and the healing parameterization, you are right that this remains an open question. As mentioned in section 4.3.2, we used the simplest possible parameterization for healing (using a constant healing rate) in the present uncoupled implementation of the Maxwell-EB model. We did not verify the validity of our approach with respect to entropy. In a dynamic-thermodynamic sea ice model, the rate of healing should logically be a function of the local difference between the temperature of the air near the surface of the ice and the freezing point of seawater below (see section 4.3.2). However we believe entropy is hard, perhaps impossible, to quantify and monitor in the context of an *open*, dynamically and thermodynamically coupled system such as the Arctic Ocean.

MINOR COMMENTS

p.2 l.6 (and many other places): "constitutive relationship:" Even though admittedly a constitutive relationship sounds very romantic, I guess the more common terminology in this context is "constitutive relation."
We replace this formulation by "constitutive law".

p.3 l.25 "physically consistent with observed behavior:" Is it physically consistent, or consistent with observed behavior, or both? In either case, that should be made clear.
It is naturally both, as something that is physically consistent should necessarily be consistent with observation. We replace this sentence by: "consistent with its observed mechanical behaviour".

p. 5 l.9 "processing... method:" I am not sure whether "processing" is the right word for this.
"Processing" is synonym of "treating" here, or "representing". We rephrase: thereby treating discontinuum mechanics with a continuum mechanics method.

p. 5 1.11 "continuum solid:" Shouldn't this be a "continuous solid?"
OK.

p.5 l.25-p.6 l.2: Maybe make two sentences out of this in order to make it more readable.
OK.

p.6 l.5: "material's velocity" rather "the velocity of the material" (as the material is not a person).
OK.

p.6 l.13f: "the ration of ... and of the time": drop second "of"
OK.

OK.

Here we make the distinction between the part of the intermittency that is attributable to the forcing applied on the material and the part that is inherited from its mechanical behaviour. This is an important difference in the context of sea ice. The turbulent wind forcing itself exhibits some intermittency, which is "transmitted" to the ice cover. This part of the intermittency is therefore expected to be reproduced in most sea ice models. However, it was shown that the wind forcing is less intermittent than the deformation of sea ice, hence that the "extra" intermittency of sea ice deformation is attributable to its mechanical behaviour (*Weiss, 2008; 2013*). It is this part of the intermittency of the deformation that cannot be adequately reproduced in sea ice model if elastic interactions are not accounted for and if the memory of elastic stresses is not adequately retained.

It refers to the previous sentence: to a rheological model that has "the capacity to distinguish between reversible and irreversible deformations" and that "allows a passage between the small/elastic and large/permanent deformations". We try improving the reading by adding "that" after "such a model".

Once again, here we do not mean to model the classical bulk viscoelasticity of ice (see response to major comment above). Viscous creep is negligible in the deformation of sea ice, which is essentially brittle (e.g., *Weiss et al., 2007*). The apparent viscosity introduced here is intended to represent the slow relaxation of elastic stresses through permanent, large deformations of the damaged material: this is why we make a parallel with models of lithospheric faulting rather than with viscoelastic models for glacier ice.

See above.

Yes, the strain rate tensor is the rate of the strain tensor and hence is the symmetric gradient of the velocity. We clarify this point by defining the strain rate tensor in equation (1) as the symmetric gradient of the velocity. *Large deformations* in the Maxwell-EB model are accounted for by introducing the objective derivative of the stress tensor in the constitutive law (eqn. 1). To clarify this point further, we include the definition of the objective material derivative for the stress tensor after introducing the constitutive relation and develop the β_a term, which accounts for the effects of rotation. It is important to recall however that all simulations presented in the paper are in the small-deformation regime (no advection and rotational effects neglected), hence these distinctions do not apply here.

Besides, we recognize that the notations used to describe the standard Maxwell model at the beginning of section 4.1 were rather confusing, especially when referring to figure 1(a) and (b) to introduce these concepts. For instance, G was used for the elastic modulus and τ was used for the stress tensor in the text and in figure 1a, instead of E and σ in figure 1b. Hence we slightly reformulated the description of the standard Maxwell model and changed the notation in figure 1(a). We believe this improves the reading and presents the transition from the standard to the Maxwell-EB model more clearly.

This definition of the (adimensional) elastic stiffness matrix is quite standard. Hence we do not think this ought to be listed as a separate equation. But we reformulate this definition in index notation, which makes it somewhat easier to grasp.

OK.

We are not sure we understand this comment. On the one hand, in the elastic regime, the effective stress is given by $\frac{\sigma}{d}=E^0\varepsilon$ with $0<d\leqslant 1$, which is consistent with the typical interpretation of damage in progressive damage models for elastic materials. On the other hand, in the viscous regime, the effective stress is given by $\frac{\sigma}{d^\alpha}=\eta^0\dot{\varepsilon}$ which does contrast with the classical definition of the effective stress due to the introduction of the damage parameter (exponent α). This viscous term does not represent a true viscous flow of the bulk material, but instead an apparent viscosity aimed at slowly relaxing the elastic stresses within a damaged material. Hence the notion of effective stress is not entirely relevant here. As the parameter α is larger than 1, our formulation means that damage plays a stronger role on the apparent viscosity than the effective stress concept would do. We agree that this point might have been confusing, especially as we state about the damage variable "This variable is interpreted as a measure of sub-grid cell defects or crack density (*Kemeny and Cook, 1986*) and is allowed to evolve (...)" (p. 15, lines 14-16). Hence we reformulate this passage as "This variable is interpreted as a measure of sub-grid cell defects".

p.13 l.22f: Please define *h*.
Thanks for catching this: *h* stands for the ice thickness.

p.14 l.22: "Time steps" and "elements" are concepts of numerical methods. One should be careful with using them for motivating the governing equations of a model. In physics, space and time are not discrete.
Here the space and time discretizations do not "motivate" the governing equations of the model, although they need to be taken into consideration when writing the continuous form of the damage equation (that is, the part of the evolution equation for *d* pertaining to the damaging process). As already discussed in this section, this arises because of our treatment of the damage mechanism, which is similar to that of linear-elastic progressive damage models (e.g *Amitrano, 1999*). The governing equation for this discrete process is written as a recursive relation (formerly on line 20, p. 15 and now numbered).
In the linear-elastic damage mechanics model on which the Maxwell-EB model is based, time does not enter the governing equations (e.g., *Amitrano, 1999*, and *Girard, 2010*), hence the formulation of an evolution equation for this mechanism is not an issue and the damage equation is simply written in this recursive form. Here evolution equations are written and as the damage process is tied to the space and time discretizations, the order of the time scheme and spatial and temporal resolutions need to be taken into account when writing the recursive equation *in continuous form*. We agree that this might constitute a limitation of the current Maxwell-EB model, especially as it requires the use of an explicit time-stepping scheme for the damage evolution and the use of a small model time step.

p.15 l.1: Equation numbers missing? Please give a clear definition of epsilon (particularly in the context mentioned above, strains and strain rates).
OK, we numbered this equation and defined epsilon, the *strain* tensor.

p.15 l.6: Again, principal stresses are not stress components (they do not have the transformation properties of tensor or vector components).
OK.

p.17 l.10: It may be overly rigorous, but I think it is not a proper use of the Landau notation to write O(some constant number)
We rewrite these formulations in words instead.

p.17 l.19: "modelling," vs. e.g. p.16 l.15, "parameterizations:" It is better style to consistently use either British or American spelling.
As the first author is Canadian, Canadian english conventions were used (which combines that of American and British spelling).

p.18 l.3: "the the"
OK.

p.18 l.23: "... are entirely defined by ... :" Either they are well-defined or not, there is nothing in between, so no need for this emphasis. Maybe better rephrase to "... only depend on"
OK.

OK.

As mentioned on lines 13 to 15, p. 19, this formulation is introduced to ensure mathematical consistency, i.e., so that the constitutive equation be defined in the limit of $d = 0$. It is not meant to handle the physical interpretation of damage in the limit of a "completely damaged" material. We mentioned this point with the intend of being as rigorous as possible, as it is how the damage equation is written in our numerical scheme. However, as also pointed out, the use of a "regularization technique" for $d = 0$, as well of this specific technique (as opposed to introducing a minimum value on d instead of on η) has no impact on our results, as the level of damage d never reaches zero values (we set $d^0 > 0$ in all simulations). Hence we agree that introducing this level of precision within the description of the governing equations might not be necessary in the present paper. We suggest to remove this entire paragraph. To take care of any ambiguities, we specify the condition $0 < d^0 = d(t = 0) \leq 1$ in the equations for E and η as a function of d (end of former page 18). We modify figure 3 accordingly and reformulate lines 13 and 14, p. 13, as "The level of damage is equal to 1 for an undamaged material and *approaches* the value of 0 in the case of a "completely damaged" material."

This sentence was cut (see above).

The 2-dimensional plate assumption here is equivalent to the plane-stress assumption, in the sense that we assume no stresses in the z direction (σ_{13}, σ_{31}, σ_{23}, σ_{32}, σ_{33} = 0). In this case, the (adimensional) elastic stiffness tensor $\boldsymbol{K}$ is defined such that for all symmetric tensor

$$\boldsymbol{\varepsilon} = \varepsilon_{ij} \, \forall i,j; 1 \leqslant i, j \leqslant 2, \boldsymbol{K}: \varepsilon_{ij} = \frac{\nu}{1-\nu^2} \varepsilon \delta_{ij} + 2 \frac{1}{2(1+\nu)} \varepsilon_{ij}.$$

However, one difference is that, as in all regional and global sea ice models, the *z-components* of the deformation are not taken into account here (the sea ice momentum balance equation is 2-dimensional). Hence yes, the velocity field is calculated in the horizontal plane (u_x, u_y) only.
This assumption was listed independently of the constant healing rate assumption. We reformulate this sentence as: "As in regional and global sea ice models, the ice cover is considered as a 2-dimensional plate due to its very large aspect ratio and plane stresses are assumed. A constant healing rate is used".

It is now replaced by "represents".

Yes, the internal stress refers to the in-plane stress, σ. In virtually all sea ice models based on the continuum assumption, it is the common name for the stress arising from the sum of the mechanical interactions between ice floes (*Weiss, 2013*, *Feltham, 2008,* and many others). It is thereby distinguished from *external stresses,* which is the formulation used for the skin (air and ocean) drags per unit area on the ice cover.
Here, the entire stress tensor instead of the deviatoric part is used, as the simulated material is a compressible, elastic solid.

The ice concentration is the fraction of a model grid cell covered by ice, or in other words, the surface of ice (as opposed to open water) per unit area. In the present model, it has the same definition as in virtually all continuum sea ice models developed since 1979 (i.e., since the Hibler viscous-plastic model). Hence we do not believe a lengthly definition of this variable is necessary.

p.20 l.17: Rather make two sentences out of this.
OK.

p.21 l.3: What is the reason not to write A = 1?
OK.

p.21 l.6: "c*" is the * a typo?
No, we did intent to use this symbol. This constant is usually denoted C (*Hibler, 1979*). We use $c*$ to distinguish it from the cohesion in the Maxwell-EB and EB frameworks.

p.21 l.20f: "the dynamical system... read:" should be singular ("reads").
OK.

p.22 l.11: "...parameters must evolve within..." so, they evolve while the model is running? This would change the dynamical equations. Otherwise, rather rephrase this.
We rephrase: "In order for the Maxwell-EB model to represent the intended physics, the value of these parameters must lie within a certain range".

p.22 l.14: "characteristic time for damaging" Rather write "damage evolution" instead of "damaging" (idem in several other passages).
OK.

p.22 l.23: typo "One the one hand"
OK.

p.23 l.6: "propagation of the damage:" drop the article.
OK.

p.23 l.13: "This separation.... calculations:" Somewhat weird semantics and ambiguous syntax in this sentence. The content absolutely makes sense though. Maybe rephrase this (and split into two sentences).
Agreed. The sentence has been split and reformulated as
"This separation of scales ensures that elements cannot recover by healing more strength than they have lost by damaging within one time step. In the case of sea ice for instance, excess healing would effectively entail a net growth, or thickening, of the pack, a process that should instead be accounted for by thermodynamic balance considerations. However, considering the estimates of the speed of elastic waves and of the healing rate of leads aforementioned, the sea ice cover naturally meets the condition $T_h << T_d$".

p.23 l.17: "Considering the estimates ... aforementioned:" Either write "the aforementioned estimates" or "the estimates ... mentioned before."
OK.

p.24 l.4: "over undamaged... areas:" rather "in" (idem l14).
OK.

p.24 l.13: typo "euqation"
OK.

p.24 l.15: "To get round this problem:" sounds very sloppy....
Replaced by "this issue can be dealt with by (...)"

p.24 l.21: ".. function, unnecessary:" no comma (maybe rather write "is unnecessary").
OK.

p.25 l.5: "... transmitting the damage information within the material:" Not sure whether "within" is the appropriate preposition.
We do think "within" works here.

p.25 l.6: I don't quite understand this logic... If the waves are not resolved, why should they be filtered out of the solution? Furthermore, replace "the model's solution" by "the solution of the model" (A model can be a person, just in this case for

sure it is not ;-))

Agreed: this paragraph is somewhat confusing, and not strictly necessary. Hence we cut these two sentences. The main point here is expressed in the two remaining sentences of this paragraph, which is that inertial effects and the effect of the propagation of viscoelastic waves on the stress and deformation fields can be safely neglected in most sea ice implementations of the model.

p.25 l.25: Rather "in a material..."
OK.

p.26 l.4: "time derivative for the Cauchy stress..." derivative of
OK.

p.26/27, description of the test geometry: I don't quite understand the boundary conditions. Is the velocity on the lower (short) edge set to (0, 0) or may there be a non-zero component in x-direction? Concerning the lateral boundary, in the text it says "no confinement is applied on the lateral sides" (that is, the boundary may move freely?), whereas in the sketch (Fig. 4) it says u(x,y) = 0, thus the velocity is fixed. Please clarify these ambiguities! Furthermore, if the lateral boundary is fixed, what happens to the inflowing ice mass if the ice thickness is kept constant?

The figure that was included in this submitted version of the paper was not the good one, and yes, was somewhat confusing. The current, corrected version indicates that:

(1) The velocity on the lower and upper edges of the plate is set to 0 in the *y* direction only : the *x*-component of the velocity can be non-zero.
(2) The velocity is strictly zero only on the lower-left corner of the plate (indicated by the triangle).
(3) No confinement is applied on the lateral sides, hence these boundaries may move freely. However, as these small-deformation simulations are run for a short time (until the *cumulative* applied deformation is of at most 10% -there was an error in the text [l.4, p. 27] so we corrected it- of the size of an average, *single* model element), the position of grid nodes is *not* updated in time (hence the FE spatial discretization is defined based on the initial mesh grid, i.e., is not updated in time). The lateral boundaries therefore do not "move" in the simulations presented here. We now mention this point in section 6.
(4) As deformations are small, mass-conservation is not prescribed (see page 27, first paragraph).

p.27 l.26f: "so that to be representative:" the conjunction "so that" should not be followed by an infinitive.
OK.

p.28 l.1: drop the comma.
OK.

p.28 l.10-26: Maybe move this to the literature discussion?
Agreed, we move this to the Introduction section.

p.29 l.8: "... is its strong anisotropy" would this finding not call for the use of a tensor damage variable? Please explain why a scalar damage model is sufficient.
Again, a scalar damage model is sufficient to generate large-scale anisotropy in an elastic medium. The kernel of elastic interactions and the resulting perturbation of the stress field in such a material becomes anisotropic as soon as some spatial heterogeneity in its mechanical strength, or if the applied forcing is not purely isotropic with respect to this heterogeneity or to the geometry of the experiment (see response to major comment above).

p.30 l.15 "over undamaged parts" rather "in undamaged parts?"
OK.

p.30 l.19: "spatial distribution of the damage criteria" isn't the damage criterion the same everywhere? Only its parameters vary.
If the parameters (e.g., *C*) of the damage criterion vary, then the damage threshold itself varies. Here the local damage threshold varies with the cohesion, *C*. We replace "criteria" by "threshold" here, to make this point clearer.

p.32 l.6: "we use the output of strain rate fields from simulations..." isn't it rather the output of simulations, not that of strain rate fields?
We removed "the".

p.32 l.24: "....and clusters in space ..." This seems somehow syntactically lost in the sentence?
Unfortunately, we do not understand this comment. We replaced this formulation by "localizes again".

p.34 l.9: "of the discrete failure events:" drop the article.
OK.

p.34 l. 25: "... the of damage rate are anti-correlated" something missing here?
Yes: *increments* of the damage rate.

p.35 l.6: "mean total deformation, that's a deformation rate, not a deformation.
OK.

p.36 l.7: "permanent deformations within the material" There are no deformations outside of the material, so no need to state this.
OK.

p.36 l.9 "show the Maxwell-EB model simulates...." maybe make the beginning of the subordinate clause clear by using "that". Or even better split into two sentences.
OK.

p.36 l.26: "internal stress within the material" why not just "the Cauchy stress"? Or even "the stress?" I guess there are neither external stresses, nor stresses outside of the material.
See previous comment: "internal stress" is the term used extensively by the sea ice modelling community.

p. 37 l.1: "of the material" instead of "the material's"
OK.

p.37 l.20: "carrying numerical experiments" rather "carrying out"
OK.

p.39 l.20: typo "shear faaults"
OK.

p.50, Fig. 6b,c: Excessive use of colored plots. Except for the yellow one, they all look more or less the same to me. I am probably not the only one who will have trouble distinguishing those plots: statistically, you can expect that about one out of ten male readers has a similar color vision deficiency. So it probably makes sense to use dash patterns instead, or to add plot labels.
Agreed: we switched to black and white and added markers wherever possible.

p.51, Fig. 7a (and various other figures): Are the units dimensionless? If so, this should be made clear, e.g. with the tilde notation used in the text.
Thank you for this comment: this was indeed not made clear since we forgot to mention that we dropped the "~" notation for all adimensional variables in the Results section. We now make this point clearer by adding a mention to this effect and by rearranging the order of a few sentence in section 6 (formerly section 4).

Answers to reviewer 2

GENERAL COMMENTS

We followed your suggestion and divided the introduction into an *Introduction* and a *Background* section. In particular, we also integrated the suggestion of reviewer 1 of moving the discussion of heterogeneity, intermittency and anisotropy (at the beginning of the Results section) to the Background section. We believe this helps presenting our motivations in developing this new rheological framework more clearly, as we indeed aim to create a model that is able to reproduce these (3) all-important characteristics of sea ice deformation.

This is indeed not what we implied. You are totally right on the point that stress balance can be non-local in fully viscous models, in other words that viscous deformations can redistribute stresses in a non-local manner. In our case, elastic interactions by nature redistribute the stress over *long* distances and need to be accounted for in order for the heterogeneity of deformation to be adequately represented in models of the ice pack.

Thank you very much for this comment: this is a very important point that we did not discuss, mainly to keep the paper as short as possible.

Introducing an intrinsic length scale, i.e., a correlation length, ξ, for damage that is larger than the model grid cell would indeed allow the model solution to converge. However, in the context of sea ice modelling, introducing a correlation length $\xi > \Delta x$ would not be physical, as the scale of natural heterogeneities (thermal cracks, brine pockets, etc) within the ice cover that serves as stress concentrators is much smaller than the typical model spatial resolution (on the order of a few to several kilometres). Furthermore, invariance of sea ice fracturing, as revealed from floe sizes distributions, holds down to the meter scale (*Weiss, 2003*). Hence here, disorder is introduced at the smallest available scale: that of the mesh element (through the field of cohesion, C). We believe this is the most rigorous choice in terms of representing the physics behind the deformation of the ice cover, but as a result the model solution is mesh-dependent and does not converge locally.

We agree that this point deserves a more extensive discussion in the paper. Hence we somewhat reformulated lines 15-22, page 11 and 1-7, page 12 to clarify the role of the spatial noise introduced in the model through the cohesion variable, C, and added a few line discussing non-local damage and convergence in section 5.1 (former lines 19-27, page 30, and 1-11, page 31).

See response to reviewer 1's comment above. The damage of an element is calculated such that, *just after* a local damage event, the stress state of the damaged element lies on the envelope.

I'm confused as to why a separate term for the ice concentration (A) is needed, as this seems at least partially redundant with damage. Why is it necessary to have both a concentration term and a damage term that modify both the elastic modulus and the viscosity? Isn't there some redundancy here, as a damaged fault/lead will necessarily have a reduced ice concentration? The ice concentration term seems to be simply added to the model at the very end of the model discussion, without much explanation.

We indeed did not discuss sea ice concentration in length in the paper, since the definition of the ice concentration is the same in the Maxwell-EB model as in typical continuum sea ice models (it is the ice-covered surface by unit area, hence it varies between 0 and 1). Its equation of evolution is therefore also similar to that employed in these models.

The coupling between the ice concentration and both mechanical parameters (see equations 17, 18) here was inspired from the coupling of A to the ice strength in compression parameter (P) suggested in the VP model of *Hibler* (1979) as well as from the coupling between the elastic modulus E and A suggested by *Girard et al.* (2011) and *Bouillon and Rampal* (2015).

In the case of the elastic modulus, E, this formulation represents the fact that when the ice concentration drops below about 90%, internal stresses become negligible and the ice is essentially in free drift. In the case of η, this dependence on ice concentration is consistent with the rapid decay of the apparent viscosity of granular media when decreasing their packing fraction from the close-packed limit (*Aranson, 2006*).

While concentration might indeed seem partially redundant with damage, we emphasize that the two variables represent different things, as the ice pack might be densely fractured, hence not withstand large stresses, but still retain a high concentration (for instance under convergent motion). Nevertheless, we agree that this parameterization, which we chose here so that to be consistent with the approach taken in previous sea ice models, could eventually be refined.

SPECIFIC COMMENTS

25: "or"
OK.

p 4, l 6-9: how have these VP hypotheses been found inconsisent? Can you summarize these for the reader?
The VP hypotheses have been found inconsistent in many respects, which are discussed in length in the studies cited here (*Weiss et al., 2007, Coon et al., 2007, Rampal et al, 2008*, see lines 8-9, page 3). Although discussing these inconsistencies could be pertinent here, it would also make the introduction significantly longer. Hence we chose to add only a short list of the main points at the end of this sentence (line 9, page 3) with the references to the relevant studies.

check English spelling throughout the document, a number of words are misspelled (looses instead of loses, euqation, it's instead of its, dependance, assymptotes,...)
OK.

p 10, l 20: there is some inconsistency in the text formatting of the different versions of "I" for the identity tensors
We reformulated the definition of **K** using index notation.

p 13, l 22-23: I was confused about what h is here
Thank you for catching this: h refers to the ice thickness and its definition in now defined.

p 19, l 18: might there be other contexts or model setups (e.g. realistic domains) for which the minimum value of d might come into play? The results of a damage model can be quite sensitive to this choice.
Problems, both conceptual and numerical, arise when the value of *d is* zero, which according to the evolution equation for *d* (line 20, p. 15 or equation 9) occurs if, and only if, the initial value of *d* (d^0) is set to zero. In the uniaxial experiment presented here, this problem does not arise since the experiment is started from a homogeneous, undamaged state (d^0 = 1). A regularization technique, such as the one presented in this paragraph, can be used to avoid numerical problems when d^0 is allowed to take the value of 0. Alternatively, a cutoff minimum value for *d* could be used.

As this section brings essentially useless complexity in the context of the simulations presented in this paper, we decided to remove it in the revised manuscript (see response to reviewer 1's comments).

We chose to incorporate the vertical integration of the internal in-plane stress in the momentum equation instead of defining σ as the vertically-integrated stress tensor to avoid confusion when evaluating the distance to the damage criterion, i.e., when comparing the local state of stress σ to the critical tensile stress σ_t and critical stress with respect to the Mohr-Coulomb criterion σ_c, both defined in Pascals (Nm^{-2}) as the cohesion C of the material. Defining σ as the vertically-integrated stress tensor would indeed necessitate redefining σ_t and σ_c in terms of an *effective* cohesion, $C \times h$. This approach is taken in the recently developed NeXtSIM model, based on the Elasto-Brittle rheology of Girard et al. (2011), and as this point was explained in the paper by Bouillon et al. (2015), we do not feel it needs to be discussed in length here, but we do agree that a clear reference to this paper is needed. Hence we reformulate the lines 10 to 13 as follows to explain this point more clearly:

"We assume the internal stress to be homogeneously distributed over the depth h and write the momentum equation in terms of the internal stress rather than the vertically integrated stress tensor more commonly used in the sea ice modelling community. This approach was also taken in the Elasto-Brittle model of Bouillon et al. (*NeXtSIM, 2015*), as it allows a direct comparison between the local state of stress and the critical stress (here σ_t or σ_c) when estimating the distance to the damage criterion."

We did perform sensitivity analyses on the relative values of t_d and Δt in the Maxwell-EB model. The results of such analyses however, depends on the applied forcing, domain geometry, etc, and hence is specific to each numerical experiment. Presenting the details of these analyses is therefore beyond the scope of the present paper. The remark of lines 6-9 was instead meant as a warning one should be careful and perhaps carry sensitivity analyses when using a model time step that is larger than the prescribed time of propagation of damage (t_d). To ensure numerical stability and allow for highest resolution of the elastic interactions in the Maxwell-EB simulations presented in this paper, we set $t_d = \Delta t$. As this also ensures the one to one correspondence between the progressive damage mechanism as described by the recursive relation of line 20, page 15 and the continuous form of equation 20, this appears to be the most logical choice. Hence to avoid giving the impression that Δt could be set arbitrarily larger than t_d in the model (at the cost of a sensitivity analysis) without any loss of physical rigor, we removed this sentence and slightly reformulated this paragraph.

We replace "inertial term" by the "time derivative" of the stress tensor.

It is now included in the background section.

OK.

We totally agree with this remark, and this is what we mean by "there is no *physical* scale associated with the localization of damage. Through elastic interactions, damage and deformation tend to localize at the finest scale (the mesh element)".

Perhaps we do not fully understand this comment, but we indeed introduced disorder (in the damage threshold) through the field of cohesion, set at the beginning of each simulation. We try rephrasing this line as "the initial disorder introduced in the model".

Thank you for this comment. Here we meant that damage models based on a linear-elastic constitutive law and without healing have been demonstrated to reproduce a highly heterogeneous deformation (the finding that is most relevant for our purpose). However, as these frameworks neither include a healing mechanism nor a slow relaxation of elastic stresses, the post macro-failure behaviour of these models is physically inconsistent, and only the path to the first rupture was analyzed. Here we seek to establish if the Maxwell-EB model, based on a viscoelastic constitutive law, has the same capability of reproducing a highly heterogeneous deformation in a partially damaged material (over subsequent healing-fracturing cycles). We hence reformulate these sentences to make this point clearer.

Yes, "increments", thank your for catching this.

Yes, resolution is increasing from top to bottom on this figure. However, you might get the impression that the resolution is the same between the experiments, especially at the beginning of the simulation (panels 1 and 2,) because the initial field of cohesion is the same in all simulations. That is, we use the field of C prescribed in the $N = 10$ simulation (lowest resolution, top row). This field is interpolated onto the finer resolution grids (see lines 16 to 19, p. 29) in the other three simulations. Perhaps this point was not made clear enough, hence we slightly reformulate the description of these experiments, at the beginning of section 5.1.
As for the right y-axis on panel (a), thank your for catching this.

Indeed, this figure shows one realization of the experiment. However, repeating the same scaling analysis for other realizations of the experiment gave very similar results. In this sense, averaging over several realizations did not give more insight.
This is what we meant by "Repeating the procedure for subsequent healing and damaging cycles and for multiple realizations of the experiment initialized with different cohesion fields showed a similar evolution of the rate of decrease of $\langle \dot{\varepsilon}_{tot} \rangle_l$ with l between macro-ruptures events, with values of β in the vicinity of the rupture consistent with previous EB model analyses (e.g., $\beta = 0.15 \pm 0.02$; Girard et al., 2010a)."
The figure below shows for instance the result of averaging $\langle \dot{\varepsilon}_{tot} \rangle_l$ computed as a function of the spatial scale, at five equidistant stages (as indicated on figure 7a, formerly figure 6a) between the minimum in macroscopic stress that follows the propagation of a fault (red) and the maximum that precedes the next macro-rupture (purple), over the second cycle of stress build-up and macro-rupture for 5 different realizations of the uniaxial compression experiment with a resolution of $N = 100$. The total deformation rate still shows a clear power law decrease with increasing spatial scale, with β largest for the post-macro-rupture (red) and pre-macro-rupture (purple) stages. The averaging could alternatively be done over multiple stress build-up/macro-rupture cycles of a single experiment. However, we believe that giving an appropriate description of the method for partitioning of the results in different stress build-up/macro-rupture cycles and averaging $\langle \dot{\varepsilon}_{tot} \rangle_l$ over these multiple cycles so that to present an "average" figure such as the one below instead of figure 7 would make the reading of this part of the *Results* section more dense than insightful.
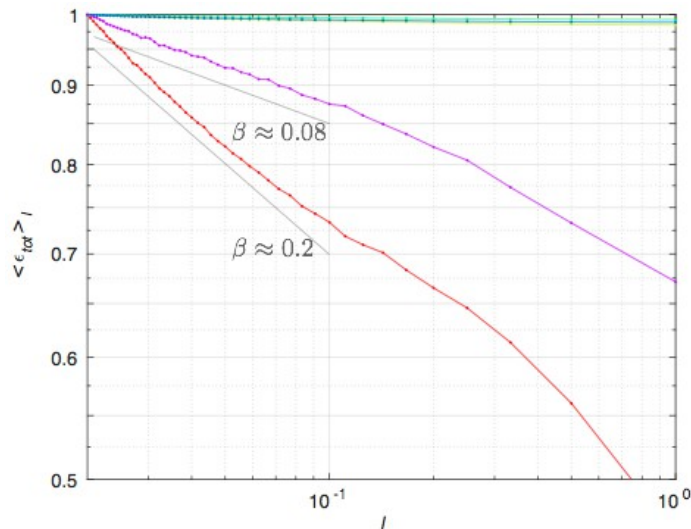
Moreover, we do not believe that *varying* the resolution would be relevant here. Increasing the resolution could indeed be interesting, in the sense that it would allow performing the scaling analysis over a larger range of space scales. Obviously it would also be computationally more expensive. Here, the analysis and the power law obtained already spans almost 2 orders of magnitude in l.

REFERENCES

Aranson, I. S. and Tsimring, L. S.: Patterns and collective behavior in granular media: Theoretical concepts, *Rev. Mod. Phys.*, 78, 641–692, doi:10.1103/RevModPhys.78.641, 2006. 8

Amitrano, D., J.-R. Grasso, and D. Hantz, 1999: From diffuse to localised damage through elastic interaction. *Geophysical Research Letters*, 26, 2109–2112.

Bažant, Z.P., Jirásek, M., 2002. Nonlocal integral formulations of plasticity and damage: survey of progress. *Journal of Engineering Mechanics,* 128 (11), 1119–1149.

Bouillon, S., and P. Rampal, 2015: Presentation of the dynamical core of neXtSIM a new sea ice model. *Ocean Modelling*, 91(0), 23–37.

Coon, M., Kwok, R., Levy, G., Puis, M., Schreyer, H., and Sulsky, D.: Arctic Ice Dynamics Joint Experiment (AIDJEX) assumptions revisited and found inadequate, *J. Geophys. Res.*, 112, C11S90, doi:10.1029/2005JC003393, 2007. 3, 13, 36

Cowie, P. A., C. Vanneste, and D. Sornette, 1993: Statistical physics model for the spatiotemporal evolution of faults. *Journal of Geophysical Research*, 98(B12), 21,809–21,821.

Eshelby, J. D., 1957: The determination of the elastic field of an ellipsoidal inclusion, and related problems. *Proceedings of the Royal Society of London A: Mathematical, Physical and Engineering Sciences,* 241(1226), 376–396.

Girard, L., J. Weiss, J. M. Molines, B. Barnier, and S. Bouillon, 2009: Evaluation of high-resolution sea ice models on the basis of statistical and scaling properties of arctic sea ice drift and deformation. *Journal of Geophysical Research*, 114(C08015).

Girard, L., Amitrano, D., and Weiss, J.: Failure as a critical phenomenon in a progressive damage model, *J. Stat. Mech.-Theory E.*, P01013, doi:10.1088/1742-5468/2010/01/P01013, 2010a. 5, 14, 16, 29, 30, 31, 32, 33

Girard, L., S. Bouillon, J. Weiss, D. Amitrano, T. Fichefet, and V. Legat, 2010b: A new modeling framework for sea ice models based on elasto-brittle rheology. *Annals of Glaciology,* 52(57).

Hibler, W. D. I., 1979: A dynamic thermodynamic sea ice model. *Journal of Physical Oceanography,* 9(7), 815–846.

Krug, J., Weiss, J., Gagliardini, O., and Durand, G.: Combining damage and fracture mechanics to model calving, *The Cryosphere*, 8, 2101–2117, doi:10.5194/tc-8-2101-2014, http://www.the-cryosphere.net/8/2101/ 2014/, 2014.

Keller, A. and Hutter, K.: A viscoelastic damage model for polycrystalline ice, inspired by Weibull-distributed fiber bundle models. Part I: Constitutive models, *Continuum Mechanics and Thermodynamics*, 26, 879–894, doi:10.1007/s00161-014-0348-7, http://dx.doi.org/10.1007/s00161-014-0348-7, 2014.

Main, I., 1996: Statistical physics, seismogenesis, and seismic hazard. *Reviews of Geophysics*, 34(4), 433–462.

Rampal, P., Weiss, J., Marsan, D., Lindsay, R., and Stern, H.: Scaling properties of sea ice deformation from buoy dispersion analysis, *J. Geophys. Res.*, 113, C03002, doi:10.1029/2007JC004143, 2008. 3, 4, 28, 35

Weiss, J.: Scaling of Fracture and Faulting of Ice on Earth, *Surveys in Geophysics,* 24, 185–227, doi:10.1023/A:1023293117309, http://dx.doi.org/10.1023/A:1023293117309, 2003

Weiss, J., 2008: Intermittency of principal stress directions within Arctic sea ice. *Physical Review E*, 77(5), 056,106.

Weiss, J., 2013: Drift, Deformation, and Fracture of Sea Ice, A perspective across scales. *SringerBriefs in Earth Sciences*, Springer Netherlands.

A Maxwell-Elasto-Brittle rheology for sea ice modelling

Véronique Dansereau[1], Jérôme Weiss[2], Pierre Saramito[3], and Philippe Lattes[4]

[1]Laboratoire de Glaciologie et Géophysique de l'Environnement, CNRS UMR 5183, Université de Grenoble, Grenoble, France
[2]Institut des Sciences de la Terre, CNRS UMR 5275, Université de Grenoble, Grenoble, France
[3]Laboratoire Jean Kuntzmann, CNRS UMR 5224, Université de Grenoble, Grenoble, France
[4]TOTAL S.A. - DGEP/DEV/TEC/GEO, Paris, France

Correspondence to: Véronique Dansereau (veronique.dansereau@lgge.obs.ujf-grenoble.fr)

1 Abstract

A new rheological model is developed that builds on an elasto-brittle (EB) framework used for sea ice and rock mechanics, with the intent of representing both the small elastic deformations associated with fracturing processes and the larger deformations occurring along the faults/leads once the ma-
5 terial is highly damaged and fragmented. A viscous-like relaxation term is added to the linear-elastic constitutive ~~relationship~~ law together with an effective viscosity that evolves according to the local level of damage of the material, like its elastic modulus. The coupling between the level of damage and both mechanical parameters is such that within an undamaged ice cover the viscosity is infinitely large and deformations are strictly elastic, while along highly damaged zones the elastic modulus
10 vanishes and most of the stress is dissipated through permanent deformations. A healing mechanism is also introduced, counterbalancing the effects of damaging over large time scales. In this new model, named Maxwell-EB after the Maxwell rheology, the irreversible and reversible deformations are solved for simultaneously, hence drift velocities are defined naturally. First idealized simulations without advection show that the model reproduces the main characteristics of sea ice mechanics and
15 deformation: strain localization, anisotropy, intermittency and associated scaling laws.

2 Introduction

Making reliable predictions of the drift and deformation of sea ice is becoming crucial nowadays for: (1) forecasting the opening of shipping routes across the Arctic, (2) evaluating mechanical constraints on offshore structures and ships and, at larger scales, (3) estimating the future evolution
20 of both the summer and winter sea ice cover in the Arctic and Antarctic to anticipate its short to long-term, regional to global impacts on climate. Current operational modelling platforms, whether assimilating data or not (e.g., TOPAZ4 : Sakov et al. (2012), GIOPS : Smith et al. (2015)), and global

1

climate models including sea ice dynamics (e.g., the Coupled Model Intercomparison Project Phase 5 models involved in the IPCC Fifth Assessment Report (Flato et al., 2013)) are based on the same

25 mechanical framework for sea ice developed in the late seventies: the Hibler Viscous-Plastic (VP) model (Hibler, 1977, 1979). With this approach, the ice creeps very slowly as a viscous fluid under small stresses and deforms plastically once exceeding a yield criterion. Yet, over the last decade, the viscous hypothesis and other underlying physical assumptions of this VP framework have been revisited and found inconsistent with the observed mechanical behaviour of sea ice., in particular

30 with respect to the order of magnitude of the observed strain-rates (Weiss et al., 2007; Rampal et al., 2008), the anisotropic distribution of ridges and leads and associated discontinuities in the velocity field on scales both small and large (> 100 km) (Hibler, 2001; Schulson, 2004; Coon et al., 2007), the relation between stresses and strain-rates (Weiss et al., 2007), the strength of pack ice in tension (Weiss et al., 2007; Coon et al., 2007) and the normal flow rule (Weiss et al., 2007). In the same

35 line of ideas, recent modelling studies have demonstrated that while the VP model can represent with a certain level of accuracy the mean, global (> 100 km) drift of sea ice, it fails at reproducing the observed properties of sea ice deformation and that, especially at the fine scales (Lindsay et al., 2003; Kwok et al., 2008; Girard et al., 2009) relevant for operational modelling, thereby stressing the need to explore alternative rheologies.

40   Other continuum models have been developed lately with the aim of representing more accurately some important aspects of the mechanical behaviour of sea ice. Considering the discontinuous and anisotropic character of the pack, Schreyer et al. (2006) have suggested an elastic-decohesive model that explicitly accounts for the deformation arising from discontinuities in displacement across leads, the orientation of which is prescribed. Tsamados et al. (2013) have presented a model based on the

45 rheology of Wilchinsky and Feltham (2006) that accounts for the subgrid scale anisotropy of the sea ice cover. Their framework incorporates an evolution equation for the orientation of ice floes, for which a diamond shape is assumed. Our present work shares the same objective as these previous initiatives : to build a continuum model for sea ice that is physically consistent with its observed mechanical behaviour. However, we chose to base our approach on a completely isotropic rheology

50 and, by incorporating the relevant brittle mechanics concepts and long-range elastic interactions, aim to develop a model that reproduces the anisotropy and extreme gradients within the sea ice cover naturally, that is, without the need of treating velocity discontinuities explicitly nor prescribing lead orientations or floe shapes.

3 Background

55 Early on, sea ice scientists have suspected that the sea ice cover ice pack behaves in a brittle instead of a viscous manner, with some strain hardening in compression (Nye, 1973). Studies In later years, studies of fracture patterns, stresses and strains both in situ and in the laboratory have suggested that

the deformation of ~~sea ice~~ the sea ice cover is mostly accommodated by a mechanism of multiscale fracturing and frictional sliding ~~. By investigating the dispersion of ice buoys, recently showed that sea ice over the Arctic deforms in a heterogenous and intermittent manner over spatial~~ (Marsan et al., 2004; Weiss et al., 2007; Schulson, 2004, 2006a). Recently, the availability of ice buoy and satellite data has allowed revealing three all-important characteristics of the deformation of sea ice: its strong localization in space, or *heterogeneity*, its localization in time, or *intermittency*, and its *anisotropy*.

On the one hand, the anisotropic nature of sea ice deformation is made evident by the analysis of satellite imagery-derived ice motion products (e.g. Stern et al., 1995), which shows that high strain rates concentrate along oriented, linear-like faults, or leads, often termed "linear kinematic features" (Kwok, 2001). The signature of the strong heterogeneity and intermittency of sea ice deformation on the other hand, is the emergence of spatial and temporal scalings in the deformation fields over a wide range of scales. Using a coarse-graining procedure, Marsan et al. (2004) performed a scaling analysis of the deformation of sea ice over the Arctic using the 3-days, $10\,\text{km} \times 10\,\text{km}$ gridded RGPS deformation product. Doing so, they obtained a power-law relationship between the total deformation rate $<\dot{\varepsilon}_{tot}>_l$ invariant and the corresponding averaging scale l of the form

$$<\dot{\varepsilon}_{tot}>_l \sim l^{-\beta} \tag{1}$$

with a constant exponent $\beta > 0$, indicating correlations in the deformation fields over at least 2 orders of magnitude in l and an increase in the mean strain rate with decreasing scale of observation, in agreement with a strong spatial localization of the deformation. This coarse-graining calculation was later extended to ice buoy data (e.g., Rampal et al., 2008; Hutchings et al., 2011) which, with a higher temporal resolution than the RGPS data, allowed performing scaling analyses of Arctic sea ice deformation in the temporal dimension as well, over space scales of 300 m to 300 km~~and time scales of~~. Using the dispersion rate of buoys as a proxy for the strain rate, Rampal et al. (2008) obtained a power-law relationship between the total deformation rate $<\dot{\varepsilon}_{tot}>_t$ computed at a chosen space scale and the time scale of observation t

$$<\dot{\varepsilon}_{tot}>_t \sim t^{-\gamma} \tag{2}$$

with a constant exponent $\gamma > 0$ over 2 orders of magnitudes in t (from 3 ~~hrs~~ hours to 3 months~~. The strong~~), indicating an increase of strain rates with decreasing time scale consistent with an intermittent deformation process. Their analyses furthermore revealed a space-time coupling ~~in the scaling laws revealed by their analyses are~~ between the spatial and temporal scaling laws, consistent with (1) a brittle-type material in which permanent deformations are accommodated by displacements along fractures and fault planes over a wide range of scales and (2) long-range elastic interactions, allowing for small, local perturbations to trigger much larger damaging events within the ice pack (Marsan and Weiss, 2010).

90   A close comparison can be made between the deformation of sea ice and that of the Earth crust, in which brittle fracturing and Coulomb stress redistribution also take place and for which scaling properties have been recognized for years (Kagan and Knopoff, 1980; Kagan, 1991; Kagan and Jackson, 1991; King et al., 1994; Turcotte, 1992; Stein, 1999). Recently, Marsan and Weiss (2010) established a formal analogy between the mechanical behaviour of sea ice and that of the Earth

95   crust by demonstrating that the space-time coupling in the deformation of sea ice, estimated from *continuous* displacement fields, is equivalent to a coupled scaling of the *discrete* ice-fracturing events occurring along the leads, similar to that observed for earthquakes (Kagan, 1991; Kagan and Jackson, 1991). The authors suggested that the similarity between sea ice and the Earth crust is attributable to a common cascading mechanism of earth-/ice-fracturing events that extends the influence of local

100 events to longer durations and larger areas than their direct aftershocks.

In the case of rocks, attempts to simulate brittle deformation were first made using random spring-like models. Combining local threshold mechanics and long-range elastic interactions, these successfully reproduced the strong localization of rupture in both space and time, the clustering of rupture events along faults and the multifractal properties of strain fields (Cowie et al., 1993, 1995). Build-

105 ing on similar linear-elastic laws and introducing some strain softening at the micro scale, the failure model of Tang (1997) succeeded in simulating the progressive failure leading to the macroscopic non-linear behaviour of brittle rock, thereby ~~processing discontinuum mechanics by a continuum mechanics method~~ treating discontinuum mechanics with continuum mechanics methods. An analogous approach based on local damage evolution was also taken by Amitrano et al. (1999), who

110 combined

- a linear-elastic constitutive ~~relationship for a continuum~~ law for a continuous solid,

- a local Mohr-Coulomb criterion for brittle failure,

- an isotropic progressive damage mechanism for the elastic modulus described by a non-dimensional scalar damage parameter, allowing for the redistribution of the stress from over-

115 critical to sub-critical areas of the material, for the triggering of avalanches of damaging events and the for propagation of faults.

This rheological framework, named Elasto-Brittle (EB), was recently developed in the context of the Arctic ice pack by Girard et al. (2011) to explicitly introduce brittle mechanics concepts in continuum sea ice models. First implementations of this rheology into short (3-days), no-advection,

120 stand-alone simulations of the Arctic, but using realistic wind forcing from reanalyses, showed that the EB model is able to reproduce the strong localization and the anisotropy of damage within sea ice and agrees very well with the deformation fields estimated from the RADARSAT Geophysical Processor System (RGPS) data (Girard et al., 2011).

4

In the context of longer-term simulations of ice conditions and coupling to an ocean component,

125 a suitable sea ice model however needs to represent not only the small deformations associated with the fracturing of the pack, but also the permanent deformations occurring once it is ~~fragmented and undamaged~~ fractured and fragmented. When ice floes move relative to each other along open leads, ~~as~~ these much larger deformations set the advective processes and overall drift pattern of the ice cover.

130 This last point is an important and intrinsic limitation of the EB framework, since the linear-elastic constitutive law does not allow solving for the elastic (reversible) and permanent deformations ~~of the simulated material separately.~~

separately. Hence to estimate the ~~material's velocity~~ velocity of the simulated material, assumptions about the amount of reversible versus irreversible deformation need to be made in the EB

135 model. The partitioning is bounded by two limit cases. (1) If a loading stress is applied to the damaged material (see Fig. 1b, dashed blue loading path) and all of the resulting deformation is assumed elastic, the material goes back to its initial position if unloaded and its velocity is zero (red dashed unloading path). This assumption was made in the no-advection simulations of Girard et al. (2011). (2) Alternatively, if all of the resulting deformation is considered permanent, the material keeps its

140 final position if unloaded (Fig. 1b, purple dashed unloading path) and the velocity is trivially estimated as the ratio of the total deformation and ~~of~~ the time associated with the loading. In the case of sea ice, the second assumption might be justified by the fact that elastic deformations within an undamaged pack are small compared to the permanent deformations associated with the opening, closing, and shearing along leads. Considering the maximum in-situ values of shear stress of 10^5

145 Pa reported by Weiss et al. (2007) and an undamaged elastic modulus between 1.0 and $10.0 \cdot 10^9$ Pa (Timco and Weeks, 2010), upper bound values for shear strains in a one meter thick elastic ice pack would be on the order of 10^{-5}. On daily time scales, these are at the lower bound of RGPS deformation rate estimates (between 10^{-4} and 10^0 day^{-1}, for Marsan et al. (2004); Girard et al. (2009)), suggesting a dominant contribution of irreversible deformations. This second assumption

150 is taken in the recently developed neXtSIM sea ice model, which is based on the EB rheology and does represent advective processes over the Arctic (Bouillon and Rampal, 2015). However, in this all-permanent deformations limit, internal stresses are immediately dissipated, hence the memory of the stresses associated with elastic deformations is erased whenever the applied loading is removed or reset. Without carrying the history of previous stresses, the model cannot exhibit the intermittency

155 intrinsic to the mechanical behaviour of sea ice, ~~i.e.,~~ that is, the part of the intermittency that is not directly inhered from the wind forcing (Rampal et al., 2009). In order to estimate adequate drift velocities, a suitable rheological model must therefore have the ~~capacity~~ capability to distinguish between reversible and irreversible deformations.

The goal of this work is to develop such a model ~~allowing~~ that allows a passage between the

160 small/elastic and large/permanent deformations and with the capability of damage mechanics models

5

to reproduce the observed space and time scaling properties of sea ice deformation. Our approach consists in introducing a viscous relaxation term into the linear-elastic constitutive law of the original EB framework. The new constitutive ~~relationship~~ law takes the form of the Maxwell viscoelastic model. The all-important difference with respect to the Maxwell framework however is that the viscosity associated with the stress dissipation term is not meant to represent the viscoplastic creep of bulk ice (Duval et al., 1983), but instead is an "apparent" viscosity that depends on the local level of damage and concentration of the ice cover. As the elastic modulus, this mechanical parameter is coupled to the progressive damage mechanism through a scalar variable d representing the time and space-evolving level of damage of the ice pack. The coupling is designed so that stresses induce elastic strains over undamaged portions of the ice and are dissipated through permanent deformations where the pack is highly fractured.

The use of a viscoelastic rheology and apparent viscosity in the case of sea ice can be supported again by the similarity between the mechanical behaviour of the ice pack and that of the Earth crust and by the existence of similar approaches to model lithospheric faulting. Active faults in the Earth crust have been known to deform in two distinct ways: either abruptly, causing earthquakes, or in an transient, aseismic manner (Scholz, 2002; Gratier et al., 2014; Cakir et al., 2012; Cetin et al., 2014). Similar to sea ice, co-seismic fracturing activates aseismic creep, leading to deformations that can be much larger than that associated with the fracturing itself and to the relaxation of a significant amount of elastic strain (Cakir et al., 2012; Cetin et al., 2014). A further justification of the introduction of such pseudo-viscosity comes from the rheology of granular media. As sea ice along leads (see Fig. 3), rocks along active faults are highly fragmented. Sheared granular media flow in a viscous manner when inertial effects can be neglected (Jop et al., 2006) with an apparent viscosity diverging as the packing fraction approaches the close-packed limit (Aranson and Tsimring, 2006). This last point will justify the dependence of our apparent viscosity on sea ice concentration.

Viscous-elastic rheological models ~~using apparent viscosities~~ combined with damage mechanics have already been used to model the deformation ~~of rock-like materials.~~ and failure of glacier ice (e.g., Keller and Hutter, 2014), particularly in the context of glacier crevassing (Pralong and Funk, 2005) and ice sheet calving (Borstad et al., 2012; Krug et al., 2014). However, the time scales involved in damage and deformation are widely different between the sea ice cover and glaciers and the processes at play are of fundamentally different nature : sea ice deforms "rapidly" under the action of the wind and ocean drags, in the brittle regime, while glaciers deform slowly, through viscoplastic deformation of bulk ice. In viscoelastic models for glaciers and ice sheets, the viscosity is therefore the dynamical viscosity associated with the true creep of polycrystalline ice. Besides, in such models damage impacts the viscous flow through the concept of effective stress.

In comparison, viscous-elastic models developed for lithospheric faulting somewhat share more similarities with the approach presented here for sea ice, especially with respect to the use of an apparent viscosity. Lyakhovsky et al. (1997) for instance built a viscoelastic damage rheology model

with the intent of representing the different stages of geological faulting, from subcritical crack growth to increasing crack concentration and material degradation, macroscopic brittle failure, post

200 failure deformation and healing. However, the evolution of damage in their model was derived from energy conservation principles rather than from a brittle failure criterion and was coupled to the elastic modulus only. ~~successfully simulated strain localization during lithospheric extension using an elasto-visco-plastic model together with an ad hoc viscosity. As their work was concerned with the ductile rather than the brittle deformation regime, strain softening in their model did not~~

205 ~~involve a progressive damage mechanism but instead was achieved by coupling the viscosity to the accumulated strain and the elastic modulus of the material was kept constant.~~ Hamiel et al. (2004) modified ~~the coupled linear elasticity and progressive damage rheological framework of~~ this rheological framework with a non-linear damage-elastic moduli relation and by adding a damage-dependent Maxwell-like viscous term to account for the gradual accumulation of irreversible strain

210 observed in typical rock mechanics experiments. The addition of this term had however a fundamentally different purpose than in the present approach in that it was intended for the representation of the small pre-macroscopic brittle failure deformations, not to bridge between small and large deformations.

To our knowledge, it is ~~therefore~~ the first time a viscoelastic Maxwell constitutive law is coupled

215 to a progressive damage (and healing) mechanism through *both* the elastic modulus and an apparent viscosity with the intent of reproducing the small deformation associated with brittle fracturing and the large, permanent post-fracture deformation of geomaterials. It is certainly the first time such a rheological model has been adapted for sea ice modelling.

The paper is structured as follow: the Maxwell-EB rheological framework is described in section

220 4. A dynamical Maxwell-EB sea ice model is presented in section 5 along with its adimensional version and a discussion of the important non-dimensional numbers involved in the model. The numerical scheme employed in the case of small-deformation experiments is presented and idealized model simulations are described in section 6. In section 7, these simulations are analyzed and discussed on the basis of the macroscopic behaviour and convergence properties of the model and

225 of the heterogeneity, anisotropy and intermittency of the simulated deformation. Conclusions are summarized in section 8.

4 The Maxwell-EB model

4.1 Constitutive ~~relationship~~law

~~The Maxwell rheology describes the~~ In 1867, James Clerk Maxwell presented a linear model to

230 describe the macroscopic behaviour of a continuum material~~exhibiting~~, typically an incompressible fluid, that exhibits both elastic and viscous properties ~~and~~ in small deformations (Maxwell, 1867).

7

This linear model combines a Newtonian viscous fluid-like damper and an elastic term and is represented schematically in one dimension by a spring and dashpot connected in series (see Fig. 1a). Considering the material as being isotropic at the elementary scale for both elastic and viscous properties, the Maxwell constitutive law reads

$$\frac{1}{E}\frac{D\sigma}{Dt} + \frac{1}{\eta}\sigma = 2\dot\varepsilon \tag{3}$$

with σ, the stress tensor, E and η the elastic modulus and viscosity of the material associated to the spring and dashpot components respectively and $\dot\varepsilon$ the strain rate tensor.

$$\frac{D\tau}{Dt} = \frac{\partial\tau}{\partial t} + (\mathbf{u}\cdot\nabla)\tau + \beta_a(\nabla\mathbf{u},\tau)$$

When a stress σ is applied to the Maxwell system, the resulting deformation ε_{total} is split between two components: the instantaneous, reversible, deformation of the spring, ε_E, and the permanent deformation of the dashpot, ε_ν, increasing linearly in time (see Fig. 1a). For a given total deformation applied to the system, the rate of dissipation of the associated stress through the permanent deformation of the dashpot is determined by the ratio, $\frac{\eta}{E}$, of the viscosity of the dashpot and of the elastic modulus of the spring, E. This ratio can be interpreted as a characteristic memory time for elastic deformations : as it decreases, the material looses its capability to retain the memory of recoverable deformations.

Here we apply this idea of stress dissipation to a 2- or 3-dimensional, compressible, elastic continuous solid and formulate the following constitutive equation by adding a Maxwell-like viscous damper term to the linear elasticity (i.e., Hooke's law) constitutive law :

$$\frac{1}{E}\frac{\mathcal{D}\sigma}{\mathcal{D}t} + (\mathbf{u}\cdot\nabla)\sigma + \beta_a(\nabla\mathbf{u},\sigma) + \frac{1}{\eta}\sigma = \mathbf{K}:\dot\varepsilon(\mathbf{u}) \tag{4}$$

where $\dot\varepsilon$ is the strain rate tensor, here equivalent to the rate of strain tensor and given by $D(\mathbf{u})=\frac{\nabla\mathbf{u}+\nabla\mathbf{u}^T}{2}$, with the velocity $\mathbf{u}$. The (dimensionless) elastic stiffness tensor $\mathbf{K}$ is defined in terms of ν, the Poisson's ratio, such that for all 3-dimensional symmetric tensor $\epsilon = \epsilon_{ij}\ \forall\, i,j;\ 1\le i,j\le 3, (\mathbf{K}:\epsilon)_{ij}=\frac{\nu}{(1+\nu)(1-2\nu)}\mathrm{tr}(\epsilon)\delta_{ij}+2\frac{1}{2(1+\nu)}\epsilon_{ij}$. In the case of large deformations, the material derivative of the Cauchy stress tensor σ takes the form

8

of the objective Gordon-Schowalter derivative (Saramito, 2016)

$$\frac{\mathcal{D}\sigma}{\mathcal{D}t} = \frac{\partial \sigma}{\partial t} + (\mathbf{u} \cdot \nabla)\sigma + \beta_a(\nabla \mathbf{u}, \sigma) \tag{5}$$

where the additional term β_a accounts for the effects of rotation and deformation on the evolution of the stress tensor and expresses as

$$\beta_a(\nabla \mathbf{u}, \sigma) = \sigma W(\mathbf{u}) - W(\mathbf{u})\sigma - a\left(\sigma D(\mathbf{u}) + D(\mathbf{u})\sigma\right)$$

with ~~I the second rank identity tensor~~ $D(\mathbf{u})$ the symmetric and ~~I the symmetric~~ $W(\mathbf{u}) = \frac{\nabla \mathbf{u} - \nabla \mathbf{u}^T}{2}$ the anti-symmetric part of the ~~fourth rank identity tensor~~velocity gradient. In this rheological framework, the mechanical parameter η is *not* the true dynamic viscosity of the material but rather is an "apparent" viscosity. The related relaxation time, $\lambda = \frac{\eta}{E}$, characterizing the rate at which internal stresses dissipate into permanent deformations, is assumed equal for both the volumetric and deviatoric components of the deformation of the compressible material.

4.2 Damage criterion

In agreement with in-situ stress measurements (Weiss et al., 2007), and as in the original EB model, the damage criterion in the Maxwell-EB rheology is based on the Mohr-Coulomb (MC) theory of fracture. In terms of the principal ~~stress components~~ stresses σ_1 and σ_2, and using the rock mechanics convention that compressive stresses are positive, the MC criterion reads

$$\sigma_1 = q\sigma_2 + \sigma_c \tag{6}$$

(or $\sigma_2 = q\sigma_1 + \sigma_c$, by symmetry of the criterion along the ~~the~~ $\sigma_1 = \sigma_2$ axis - see Fig. 2). The slope of the envelope in the principal stresses plane, q, is expressed in terms of the internal friction coefficient μ as

$$q = \left[(\mu^2 + 1)^{1/2} + \mu\right]^2. \tag{7}$$

The intercept σ_c of the MC criterion with the σ_1 axes (see Fig. 2), interpreted as the uniaxial (unconfined) compressive strength, is given by

$$\sigma_c = \frac{2C}{\left[(\mu^2 + 1)^{1/2} - \mu\right]}. \tag{8}$$

with the cohesion C setting the local resistance of the material to pure shear. Disorder is introduced in the damage criterion through a noise in the spatial distribution of C. This noise represents the ~~material's natural heterogeneity that causes progressive failure behaviour~~ natural heterogeneity of a real material associated with various structural defects serving as stress concentrators and which causes the progressive failure of the material even under homogeneous forcing conditions ~~and is~~

~~associated with structural defects at the sub-grid scale, thermal cracks in sea ice for instance, serving as stress concentrators . No correlation length is associated to these heterogeneities, hence their spatial scale corresponds to the~~ (e.g., Herrmann and Roux, 1990; Amitrano et al., 1999; Tang, 1997). In the case of the ice pack, heterogeneities arise for instance in the form of thermal cracks or brine pockets (Schulson, 2004; Schulson and Duval, 2009), the length scale of which is much smaller than the typical spatial resolution of ~~the model,~~ models (≥ 1 km). Therefore, heterogeneity in the Maxwell-EB model is introduced at the smallest resolved scale, that is the mesh element size Δx~~,~~ ~~and~~, by drawing randomly the value of C over each ~~model element is drawn randomly~~ element from a uniform distribution of values spanning estimates from in-situ stress measurements in Arctic sea ice (Weiss et al., 2007). The internal friction coefficient μ is set to 0.7, a value seemingly scale-independent and consistent with laboratory experiments on Coulombic shear faults in fresh ice (Schulson et al., 2006b; Fortt and Schulson, 2007; Weiss and Schulson, 2009) and also common for geomaterials (Byerlee, 1978; Jaeger and Cook, 1979).

For metals and rocks, the MC theory was shown to be defective in the case of tension (Paul, 1961), as the mechanism of tensile failure is intrinsically different to that of compressive failure and, in general, does not involve friction. In the case of $\sigma_1, \sigma_2 < 0$, fracture occurs whenever σ_1 or σ_2 reaches a critical value. However, in-situ stress measurements in Arctic sea ice have revealed that pure tensile failure does not significantly modify the Coulombic-like failure envelope of pack ice and that Coulomb branches well describe this envelope even under large tensile stresses, up to at least $\sigma_N \sim 50$ kPa (Weiss et al., 2007). Here, we therefore extend the Mohr-Coulomb criterion to tensile stresses and for practical reasons, set the critical value to the ultimate tensile stress σ_t, defined as the intersection of the Mohr-Coulomb criterion with the σ_2 axis (Paul, 1961), as shown on Fig. 2. The tensile strength cutoff therefore takes the form:

$$\sigma_1 < 0; \; \sigma_2 = \sigma_t, \tag{9}$$

where

$$\sigma_t = -\frac{\sigma_c}{q} = -2C\left[(\mu^2+1)^{1/2} + \mu\right]. \tag{10}$$

This gives a ratio of the ultimate tensile stress and uniaxial compressive stress of $\frac{\sigma_t}{\sigma_c} \approx 0.27$, which might slightly overestimate the tensile strength for sea ice as measured on the field (Weiss et al., 2007) and in the lab (Schulson, 2006a) ($\sigma_t \approx 0.2\sigma_c$). However, as such large values of tensile strength are rarely obtained in the Maxwell-EB model simulations, this choice does not significantly affect our results.

No truncation to the MC criterion is used to close the envelope towards biaxial compression (i.e., beyond σ_c) as instances of large biaxial compressive stresses are seldom encountered in Arctic sea ice (Weiss et al., 2007). Besides, imposing a truncation was shown to have little impact on the simulation results. The damage criterion combining the MC envelope and the tensile strength cutoff

is represented in Fig. 2 in the principal stresses plane and has the same shape as deduced by Coon et al. (2007) from measurements in undamaged pack ice.

4.3 Progressive damage mechanism and healing

330 The Maxwell-EB rheology differs from the standard Maxwell rheology in that the mechanical parameters E, η and λ are not constant but all coupled to the spatially and temporally evolving level of damage of the material, which controls its local degradation and re-increase in strength. Consistent with previous damage rheological frameworks, the level of damage is represented by a non-dimensional, scalar parameter d~~evolving between~~ . The level of damage is equal to 1 ~~(undamaged~~

335 ~~) and~~ for an undamaged material and approaches the value of 0 ~~(~~in the case of a "completely damaged" material~~)~~. This variable is interpreted as a measure of sub-grid cell defects ~~or crack density~~ and is allowed to evolve through two competing mechanisms : damaging and healing. On the one hand, damaging represents fracturing and the opening of faults, or "leads" in the case of sea ice, occurring when and where the internal stress exceeds the mechanical resistance of the material and

340 which leads to its weakening. Healing on the other hand represents the reconsolidating and strengthening of the damaged material through sintering or, in the case of sea ice, refreezing within open leads. Although this mechanism also contributes to the increase in elastic stiffness ($E \times h$, with h the ice thickness) and effective apparent viscosity ($\eta \times h$) of the ice, healing is distinguished from pure thermodynamic growth or dynamically-driven thickness redistribution (e.g., Rothrock, 1975)

345 in that it applies only where and when the material has been damaged. It therefore allows d, E and η to re-increase at most to their undamaged value; $d^0 = 1$, E^0 and η^0 respectively. Because the two processes operate simultaneously within the simulated material, an evolution equation for d needs to include both mechanisms. In the following damaging and healing are first treated separately and then combined in a single equation for d.

4.3.1 Damaging

Contrary to typical sea ice modelling frameworks, no plastic (i.e., normal) flow rule is prescribed when the damage criterion is reached in the Maxwell-EB model. Instead, when the stress locally exceeds the critical stress, the elastic modulus is allowed to drop, leading to local strain softening (e.g., Amitrano et al., 1999; Cowie et al., 1993; Tang, 1997; Hamiel et al., 2004, and others). Because of

355 the long-range interactions within the elastic medium, local drops in E imply a stress redistribution that can in turn induce damaging of neighbouring elements. By this process, "avalanches" of damaging events can occur and damage can propagate within the material over long distances (Amitrano et al., 1999; Girard et al., 2010). As the elastic perturbation generated by such events is anisotropic (Eshelby, 1957), this propagation mechanism naturally leads to the emergence of both spatial het-

11

erogeneity and anisotropy in the stress and strain fields, i.e., to the formation of linear-like faults (see section 7).

In the Maxwell-EB model, the *change* in level of damage corresponding to a local damage event is determined as a function of the distance of the damaged model element to the yield criterion. Three important assumptions are made when calculating this distance, denoted d_{crit}. The first is that the deformation of each model element is conserved during a damaging event, i.e., at initiation, damage modifies only the local state of stress, not strains. The second is that, for a sufficiently small model time step Δt, i.e. very small compared to the viscous relaxation time λ (see section 5.1), a negligible part of the stress is dissipated into viscous deformation. A third constraint is based on the fact that stresses outside the failure envelope are not physical because brittle failure would occur before the material could support them. Hence we consider that after being damaged, an element has its state of stress lying just on the failure envelope. With these assumptions, the following equality holds for each damaged element:

$$\varepsilon' = \varepsilon \longleftrightarrow \frac{\mathbf{K}^{-1}\sigma'}{E \times d_{crit}} = \frac{\mathbf{K}^{-1}\sigma}{E}, \tag{11}$$

~~where the~~

$$\tag{12}$$

where ϵ is the strain tensor and the superscript $'$ denotes the post-damage state of deformation and stress. In terms of the principal ~~stress components~~ stresses, the change in level of damage of a given element is given by

$$d_{crit} = \frac{\sigma_1'}{\sigma_1} = \frac{\sigma_2'}{\sigma_2}, \tag{13}$$

which implies that as the level of damage varies, all stress components vary in the same proportions. Hence the state of stress σ' after each damaging event is given by the intersection of the failure envelope and of the line connecting the pre-damage state of stress (σ_1, σ_2) with the origin, in the principal stress plane (see Fig. 2). Two cases must be distinguished when calculating σ', depending on which of the Mohr-Coulomb or tensile criterion has been exceeded. Combining the two, d_{crit} is evaluated simultaneously over all mesh elements of the model domain as:

$$d_{crit} = \min\left[1, \frac{\sigma_t}{\sigma_2}, \frac{\sigma_c}{\sigma_1 - q\sigma_2}\right]. \tag{14}$$

Following progressive damage models, the level of damage of a given element in the Maxwell-EB model at any given time is determined by both its instantaneous distance to the damage criterion d_{crit}, i.e., its current state of stress, and its previous damage level. This implies that the variable d carries the entire history of damage of model elements and, if discretizing time as $t_n = n\Delta t$, $n \geq 0$, translates into the discrete recursive equation

$$d^{n+1} = d_{crit}^{n+1} d^n, \; 0 < d^0 \leq 1. \tag{15}$$

12

A continuous evolution equation for d can be obtained by considering that the time characterizing the redistribution of stress between model elements is intrinsically tied to the speed of propagation of elastic waves, c, in the material, which carry the damage information. Using a Backward explicit scheme of order 1, and setting the model time step to $\Delta t = t_d$ with $t_d = \frac{\Delta x}{c}$, the exact time of propagation of an elastic wave with speed c over a distance Δx, the following equation arises:

$$\frac{Dd}{Dt} = \frac{d_{crit} - 1}{t_d} d. \tag{16}$$

4.3.2 Healing

By healing, the simulated material is allowed to regain some strength. The characteristic time for this process is designated in the following by t_h. It corresponds to the time required for a completely damaged element ($d = 0$) to recover its initial stiffness ($d = 1$), which in a dynamic-thermodynamic sea ice model would depend on the local difference between the temperature of the air near the surface of the ice and the freezing point of seawater below. Healing schemes of varying level of complexity could be used in the Maxwell-EB model. One possibility is the one employed in the EB sea ice model of Girard et al. (2010), which follows parameterizations of the vertical growth of sea ice (Maykut, 1986). An underlying assumption is that the rate of healing is inversely proportional to the level of damaging of the ice. However as there is no physical evidence for this assumption, in the following, uncoupled, implementation of the Maxwell-EB model we use an even simpler parameterization that implies a constant healing rate, $\frac{1}{t_h}$:

$$\frac{Dd}{Dt} = \frac{1}{t_h}, \ 0 \leq\leq d \leq 1. \tag{17}$$

Combining both the damaging and healing mechanisms (Eq. 14, 16 and 17), the complete evolution equation for d is

$$\frac{\partial d}{\partial t} + (\mathbf{u} \cdot \nabla)d = \left(\min\left[1, \frac{\sigma_t}{\sigma_2}, \frac{\sigma_c}{\sigma_1 - q\sigma_2}\right] - 1 \right) \frac{1}{t_d} d + \frac{1}{t_h}, \ 0 < d \leq 1, \tag{18}$$

Although the two processes apply simultaneously on the level of damage in the model, they are inherently distinct. On the one hand, damaging is a discrete threshold mechanism applying only ~~where and when~~ when and where the state of stress becomes overcritical. As mentioned in sections 4.2 and 4.3.1, the characteristic time for this process, t_d, is tied to the speed of propagation of (shear) elastic waves and to the model's spatial resolution. In the case of an heterogeneous ice pack, an average value for c is on the order of 500 m/s (Marsan et al., 2011). For spatial resolutions between that of current global climate and high resolution regional sea ice models (~~$\Delta x = 1$~~ $\Delta x \approx 1$ to 100 km), the characteristic time for ~~damaging~~ damage evolution, t_d therefore varies between ~~$O(1)$ and $O(10^2)$ s~~ a few seconds to a few hundreds of seconds. Healing on the other hand is a continuous

13

process acting on all model elements, independently of the local distance to the damage criteria.
Studies on the refreezing within leads in sea ice showed that the time for 1 meter of ice to grow within an opening of 10 cm under atmospheric temperatures of $T_a = -15°C$ is of ~~$O(100)$ hours or $O(10^5)$ seconds~~ a hundred hours (between 10^5 and 10^6 seconds, Petrich et al., 2007). The orders of magnitude of difference between t_h and t_d therefore imply that the two processes are intrinsically decoupled in the case of the ice pack.

4.3.3 Coupling d with E and η

The coupling between the Maxwell-EB constitutive ~~relationship~~ law and the progressive damage mechanism constitutes one of the main features of this new modelling framework. It is defined such that:

- deformations within an undamaged medium are small and reversible, i.e., strictly elastic. Hence undamaged portions of the simulated material have a maximum elastic modulus E^0 and a very large apparent viscosity η^0. In this case, the viscous term in (4) is negligible and a linear-elastic constitutive ~~relationship~~ law is recovered (Fig. 3, right panel),

- deformations can accumulate over highly damaged areas of the material to become arbitrarily large. These deformations are permanent and dissipate most of the ~~the~~ stress applied to the material within a short relaxation time. Hence the elastic modulus, viscosity and relaxation time drop locally over damaged areas. In the limit of a completely damaged material, elastic interactions are hindered and deformations are strictly irreversible (Fig. 3, left panel). In this case, $\lambda \longrightarrow t_d$ and a soft elastic-plastic behaviour is recovered in which the memory of the elastic stresses is totally lost (narrow-dashed blue line on Fig. 1).

- as damaged areas are allowed to heal, E, η and λ all re-increase, up to their initial undamaged values.

Different functions could be used to express the dependence of E, η and λ on d that meet these criteria. In the absence of physical evidences for a higher level of complexity, and consistent with the relationship between the elastic modulus and crack density used in damage models of rocks (Agnon and Lyakhovsky, 1995; Amitrano et al., 1999; Schapery, 1999), we use the simplest parameterization and set

$$E(t) = E^0 d(t) \tag{19}$$
$$\eta(t) = \eta^0 d(t)^{\alpha}, \tag{20}$$

~~such that~~

$$, \tag{21}$$

14

with $0 < d(t=0) \le 1$ such that

$$\lambda(t) = \frac{\eta^0}{E^0} d(t)^{\alpha-1} \tag{22}$$

with α a constant greater than 1 introduced to fulfil the constraint that the relaxation time for the stress also decreases with increasing damage and re-increases with healing, as the material respectively looses and recovers the memory of reversible deformations. Using this formulation, both η and E ~~are entirely defined by their initial value , a constant, and by~~ depend only on their undamaged value and on the level of damage variable d. ~~However, the constitutive equation becomes undefined in the limit of $d \to 0$. This problem can be handled by imposing a fixed minimum value $d_{min} > 0$ for the level of damage. Alternatively, a cutoff $\eta_{min} \ll \eta^0$ on the value of the apparent viscosity can be introduced and the expression for $\eta(d)$ modified as~~

$$\eta = (\eta^0 - \eta_{min})d^\alpha + \eta_{min} = \eta^0 \text{ for } d = 1, \eta_{min} \text{ for } d = 0.$$

~~Substituting for η in the expression for the relaxation time, the elastic modulus then becomes~~

$$E = \frac{\eta^0 - \eta_{min}}{\eta^0} E^0 d + \frac{\eta_{min}}{\eta^0} \frac{1}{d^{\alpha-1}} E^0,$$

~~such that $E \approx E^0$ for $d = 1$, E decreases with d until a minimum at $d(E_{min}) = \left[\frac{\eta_{min}}{\eta^0 - \eta_{min}}(\alpha - 1)\right]^{\frac{1}{\alpha}}$ and $E \to \infty$ for $d \to 0$. Using such a cutoff on η, the elastic term in the Maxwell-EB constitutive equation therefore vanishes in the limit of a "totally" damaged material and the rate of viscous dissipation is then set by the minimum viscosity η_{min}. It is important to note that this limit has no physical significance in the context of a progressive damage model for a continuum solid and is rather introduced to insure mathematical consistency while retaining a continuous function for the level of damage. In the following implementation of the model, we take this approach instead of imposing a minimum value of d, but it had really no impact on our results since in the simulations presented here $d > d(E_{min})$ at all times.~~

5 A Maxwell-EB sea ice model

In this section, the Maxwell-EB rheology is implemented in the context of sea ice modelling. As in regional and global sea ice models, the ice cover is considered as a 2-dimensional plate due to its very large aspect ratio and ~~a~~ plane stresses are assumed. A constant healing rate is ~~assumed~~used. In this case, the complete dynamical model is given by the following system of equations:

1. The momentum equation:

$$\rho h \left[\frac{\partial \mathbf{u}}{\partial t} + (\mathbf{u} \cdot \nabla)\mathbf{u}\right] = \mathbf{F_{ext}} + \nabla \cdot (h\sigma), \tag{23}$$

15

with $\mathbf{u}$ the velocity, h the thickness and ρ the density of sea ice. F_{ext} ~~assimilates~~ represents all external forces on the sea ice cover, which in regional and global sea ice models are typically the air and ocean drags and the forces associated with the Coriolis acceleration and gradients in sea surface height. We assume the internal stress to be homogeneously distributed ~~within the depth~~ over the thickness h and ~~following and , we~~ write the momentum equation in terms of the internal stress rather than the vertically integrated stress tensor more commonly used in the sea ice modelling community. This approach was also taken in the Elasto-Brittle model of Bouillon and Rampal (NeXtSIM 2015), as it allows a direct comparison between the local state of stress and the critical stress (σ_t or σ_c here) when estimating the distance to the damage criterion.

2. Conservation equations for the ice concentration A (ice-covered surface per unit area) and ice thickness h:

$$\frac{\partial h}{\partial t} + \nabla \cdot (h\mathbf{u}) = S_h, \; h \geq 0 \tag{24}$$

$$\frac{\partial A}{\partial t} + \nabla \cdot (A\mathbf{u}) = S_A, \; 0 \leq A \leq 1. \tag{25}$$

where S_h and S_A represents thermodynamic source and diffusion terms~~and~~. An assumption behind these conservation equations is that elastic compressibility effects are ~~assumed~~ negligible relative to dynamic variations of the ice volume~~in the conservation of the mass of the sea ice cover.~~

3. The constitutive ~~relationship~~ law (4) with

$$E = f_1(E^0, \eta^0, \eta_{min}, d) \exp\left[-c * (1-A)\right] d) \exp\left[-c^* (1-A)\right], \tag{26}$$

$$\eta = f_2(\eta^0, \eta_{min}, d) \exp\left[-c * (1-A)\right] d) \exp\left[-c^* (1-A)\right], \tag{27}$$

where f_1 and f_2 represent the functional ~~dependance~~ dependence on the level of damage of the ice d, given by (19) and (21) respectively. The exponential function of the ice concentration allows the internal stress term to be maximal when ~~$A = 100\%$~~ $A = 1$ and to decrease rapidly when leads open and A drops. It is of the same form as that used for the pressure term (P, or ice strength in compression) in the VP rheology of Hibler (1979). Here the non-dimensional parameter ~~$c*$~~ c^* characterizing this dependence on the ice concentration has the same (constant) value for both mechanical parameters, but could be set different in a refined parameterization.

4. The equation for the evolution of damage (18) with the damage criterion defined by Eq. (6) and Eq. (9) and q, σ_c and σ_t given by (7), (8), (10) in terms of the cohesion variable C and of the constant internal friction coefficient μ.

In the case of "quenched disorder" (i.e., when the field of C is set at the beginning of a model simulation), an additional equation arises that handles the advection of the field of cohesion with the simulated velocity field. Table 1 lists all model variables and parameters.

5.1 Characteristic numbers and times

Neglecting all thermodynamic effects and variations in ice thickness and concentration (considering $h = 1$ and $A = 100\%$) as well as external forcings and adimensionalizing with respect to the ice velocity U, the horizontal extent of the model domain L, ~~the thickness of the ice H~~ and the undamaged elastic modulus E^0, the dynamical system of equations ~~read~~ reads

$$\mathrm{Ca}^0 \frac{D\tilde{\mathbf{u}}}{D\tilde{t}} = \tilde{\nabla} \cdot \tilde{\sigma} \tag{28}$$

$$\mathrm{We}^0 d^{\alpha-1} \frac{D\tilde{\sigma}}{D\tilde{t}} + \tilde{\sigma} = \mathrm{We}^0 d^{\alpha'} \mathbf{K}(\nu) : \tilde{\dot{\varepsilon}}(\tilde{\mathbf{u}}) \tag{29}$$

$$\frac{Dd}{D\tilde{t}} = \left(\min\left[1, \Sigma_t \frac{1}{\tilde{\sigma}_2}, \Sigma_c \frac{1}{\tilde{\sigma}_1 - q\tilde{\sigma}_2} \right] - 1 \right) \frac{1}{T_d} d + \frac{1}{T_h}, \ 0 < d \leq 1. \tag{30}$$

~~where $d^{\alpha'} = \left[\left(1 - \frac{\eta_{min}}{\eta^0} \right) d^\alpha + \frac{\eta_{min}}{\eta^0} \right]$ and~~ where the superscript '~' is used for all non-dimensional variables and operators.

In this form, the model involves 8 characteristic numbers and time scales : the (undamaged) Cauchy number, We^0, the (undamaged) Weissenberg number, ν Poisson's ratio, Σ_t the dimensionless critical tensile stress, Σ_c the dimensionless critical stress with respect to the Mohr-Coulomb criterion, T_d the characteristic time for ~~damaging~~ damage evolution, T_h the characteristic time for healing and α the damage constant. In order for the Maxwell-EB model to represent the intended physics, the value of these parameters must ~~evolve~~ lie within a certain range ~~of values~~. In the following we elaborate on the absolute and relative values of those numbers which are the most critical in the context of sea ice modelling.

5.1.1 T_d

As mentioned in the previous section, the (adimensional) characteristic time for the propagation of damage, $T_d = \frac{t_d}{T}$ with $T = \frac{L}{U}$, is determined by the speed of propagation of elastic waves within the simulated material and is strongly tied to the mean spatial resolution of the model, as t_d should be of ~~O(~~order $\frac{\Delta x}{c}$ ~~)~~. In turn, this time places a strong constraint on the Maxwell-EB model time step. Setting $\Delta t < \frac{\Delta x}{c}$ is indeed unphysical, as the time associated to one model iteration would then be too short for the stress to be redistributed from one overcritical element to its direct neighbour. For the model to resolve the propagation of damage, the time step must therefore be $\geq t_d$.

No strict upper bound to Δt is imposed by the damage mechanism. ~~One~~ On the one hand, choosing $\Delta t > t_d$ could be interesting in terms of reducing computational costs. Physically, it implies

17

535   that damage is allowed to propagate beyond the first neighbour barrier and over larger distances within one model time step. On the other hand, increasing Δt with respect to t_d also implies (1) a decrease in the resolution of damaging, as the model might miss important intermediate damage events that trigger additional interactions between neighbouring elements and (2) larger local drops in the level of damage, inducing large stress perturbations and, potentially, numerical instabilities

540   in the model. ~~Sensitivity analyses on the propagation of the damage should therefore be performed when choosing $\Delta t > t_d$.~~ The temporal resolution that is optimal in terms of capturing all elastic interactions within the simulated material <ins>and ensuring numerical stability</ins> is therefore $\Delta t = t_d$. In ~~the model experiments~~ <ins>all simulations</ins> presented in the following, this is the choice we make.

5.1.2 T_h

545   In order for healing not to offset damaging in the rate of change of d, the (adimensional) time for healing, $T_h = \frac{t_h}{T}$, must be much larger than the (adimensional) time for damage propagation. This separation of scales ensures that elements cannot recover by healing more strength than they have lost by damaging within one time step~~, as~~<ins>. In the case of sea ice for instance,</ins> excess healing would effectively entail a net growth~~of the material~~<ins>, or thickening, of the pack</ins>, a process that ~~is not intended by

550   this parameterization and~~ should instead be accounted for by thermodynamic ~~, balance calculations. Considering the~~ <ins>balance considerations. However, considering the aforementioned</ins> estimates of the speed of elastic waves and of the healing rate of leads ~~aforementioned (~~<ins>(see</ins> section 4.3), ~~pack ice naturally meets this condition~~<ins>the sea ice cover naturally meets the condition</ins> $T_h \ll T_d$.

5.1.3 We

555   The Weissenberg number, We, defined as the dimensionless product of the viscous relaxation time for the stress and of time $T = \frac{L}{U}$ characterizing the deformation process:

$$\text{We} = \frac{\eta}{E}\frac{U}{L} = \frac{\lambda}{T}, \tag{31}$$

sets the viscous versus elastic character of the flow of a viscoelastic material. In the original Maxwell model, $\text{We} = 0$ represents the limit of zero elastic stresses, while a very large We characterizes a

560   strictly elastic solid. In the Maxwell-EB model, the Weissenberg number evolves according to the level of damage as $\text{We} = \text{We}^0 d^{\alpha-1}$ with We^0, its maximum value.

    As viscous dissipation should be insignificant ~~over~~ <ins>in</ins> undamaged and strictly elastic areas of the material, We^0 should be chosen very large, representing the limit of $\frac{1}{\eta^0} \longrightarrow 0$. In this case the viscous term in the constitutive ~~relationship~~ <ins>law</ins> (4) effectively vanishes and a linear elastic rheology

565   is recovered. In practice, the value of We^0 is however limited, first, by the machine precision and second, due to a numerical scheme failure known in the field of viscoelastic flow computations as the high Weissenberg number problem (Keunings, 1986; Fattal and Kupferman, 2004, 2005; Saramito,

2014). For large values of We, numerical instabilities arise in Maxwell-type models due the presence of deformation source terms (β_a) in the transport equation for the stress tensor (5). With We^0 (or equivalently, λ^0) too low, simulations can run for a time $t \sim \lambda^0$ and unphysical viscous dissipation can occur ~~over~~ in undamaged parts of the simulated material. ~~To get round this problem,~~ This issue can be dealt with by multiplying the viscous term in the Maxwell constitutive ~~relationship can be multiplied~~ law by a Heaviside function ~~d^*~~ that effectively sets $\frac{1}{\eta}$ to the limit value of 0 when and where $d \geq d_c$, with d_c a chosen threshold value (e.g., $d_c = 1$ when using a constant heal rate parameterization) and leaves the constitutive equation unchanged ~~($d^* = 1$)~~ otherwise. In small-deformation experiments, i.e., run for a time $t \ll \lambda^0$, viscous dissipation over undamaged parts of the material is not significant and the inclusion of such a function ~~,~~ is unnecessary.

Conversely, where damage becomes important, the viscous relaxation time λ should decrease significantly below the characteristic time for healing to allow for internal stresses to "have time" to dissipate and deformations to become large.

5.1.4 Ca

The dimensionless number that arises when adimensionalizing stresses in the momentum equation with respect to the elastic modulus is the Cauchy number, defined as the ratio of inertial to elastic forces (Ca $= \frac{\rho U^2}{E}$). If inertial forces are comparable to elastic forces and Ca ~ 1, the effect of the propagation of viscoelastic waves in the material cannot be neglected. ~~Yet, setting $\Delta t \geq t_d$, that is Δt at least equal to the period of shear elastic waves, implies that the model does not resolve these waves, but only their consequence of transmitting the damage information within the material. Hence the wave signal cannot be properly filtered out of the model's solution. In order for the wave contribution not to have a significant effect on the simulated deformation and stress fields, Ca must therefore be $\ll 1$.~~ Dimensional analysis indicates that over an undamaged ice pack with velocity ranging between 0.001 and 1 m/s, Ca^0 is in the range $[10^{-12} - 10^{-6}]$. Hence inertial effects can be safely neglected. For simulated ice velocities $U < 1$ m/s, and $\alpha > 2$, inertial effects in the Maxwell-EB model remain negligible when damage becomes important.

5.1.5 α

The damage parameter α controls the rate at which the apparent viscosity decreases and the material looses its elastic properties with damaging. As mentioned in previous sections, it should be set greater than 1 in order for the viscous relaxation time to decrease with damaging. The requirements that (1) the viscous relaxation time drops well below the time for healing over highly damaged areas and (2) inertial effects remain negligible for high deformation rates (i.e., large velocities) can also place a constraint on the minimum value of α. Conversely, for large values of α, the relaxation time λ becomes very small whatever the damage level (see section 4.3.3). This means that elastic

19

deformations are almost immediately dissipated after damaging, that is, the model becomes purely elasto-plastic. The sensitivity of the model to the value of this parameter was kept for a separate paper, hence α is not varied here. For the experiments presented ~~herein~~ in section 7, we find that $\alpha = 4$

605 allows representing both the brittle behaviour and the relaxation of the internal stress ~~within~~ in a material with mechanical parameters in the range of the values suitable for sea ice. For α larger than about 7, memory effects become insignificant and the experiment instead exhibits a stick-slip behaviour with a well-defined characteristic frequency (not shown).

6   Numerical scheme and experiments

610 The objective time derivative ~~for~~ of the Cauchy stress σ in the Maxwell-EB constitutive ~~relationship~~ ~~law~~ (4) is composed of ~~an inertial term~~ a time derivative, an advection term and of a sum of rotation and deformation (β_a) terms, each of which implies a different level of numerical complexity. In developing the model, our approach is to introduce each of these terms separately in order to evaluate their respective contribution to the simulated mechanical behaviour. On the one hand, introducing

615 the ~~inertial term~~ time derivative while neglecting the advection and β_a terms allows retaining a Lagrangian scheme, similar to the original EB model (Girard et al., 2011). Without any remeshing of the domain, the model is then suitable for short-term, small-deformation simulations only. On the other hand, when permanent deformations accumulate over a long time, the advection term is no longer negligible and β_a terms become potentially important.

620 In the following, we present small-deformation numerical experiments that allow analyzing the mechanical behaviour of the Maxwell-EB model in terms of the statistical and scaling properties of the simulated damage and deformation fields. Performed with a highly idealized configuration for the domain geometry, the applied loading and boundary conditions, these will demonstrate that the main characteristics of sea ice deformation (spatial heterogeneity, anisotropy, intermittency) natu-

625 rally emerge from the underlying physics and do not need to be implemented in an ad-hoc manner.

The simulations represent the uniaxial compression of a (2-dimensional) rectangular ice plate with dimensions $\frac{L}{2} \times L$ (see Fig. 4a). Compression is applied by prescribing a constant velocity U on the upper short edge of the plate with the opposite edge maintained fixed in the direction of the forcing. No confinement is applied on the lateral sides. The velocity U is set small enough to ensure a low

630 driving rate (i.e., slow compared to time scale of damage propagation, (Cowie et al., 1993)).

In the present implementation, the model is not yet coupled to a thermodynamic component, hence $S_A = S_h = 0$. As advection is neglected and simulations are run for a short enough time such that the macroscopic and local deformations within the ice cover remain small (~~$\sim 1\%$ of the area of model elements~~ the *cumulative* deformation is $\leq 10\%$ of the size of a single model element), dynamics-

635 induced variations (through convergence-divergence) of the ice thickness and concentration are not

accounted for and hence the mechanical parameters E, η and C are not yet coupled to h or A. Conservation of mass is therefore not imposed in these small-deformation simulations, equivalent to assuming a uniform, constant thickness (1 m) and ice concentration (100%). ~~In this case, the system of equations reduces to Eq. to with $\frac{D\tilde{\mathbf{u}}}{D\tilde{t}} = 0$ and the 6 unknowns $\tilde{\mathbf{u}}$ (2 components), $\tilde{\sigma}$ (3 components) and $\tilde{d}$.~~ All simulations are started from an initially undamaged ice cover with uniform elastic modulus and viscosity. Undamaged mechanical parameter values are chosen to represent sea ice on regional to global scales ($c = 500\,\mathrm{ms}^{-1}$ and $\nu = 0.3$). The undamaged elastic modulus is given by the relation $E^0 = 2c^2(1+\nu)\rho$ and the undamaged viscosity η^0 is set such that the initial relaxation time λ^0 is as large as possible while the maximum Weissenberg number We^0 is small (<1). All model variables and parameters are listed in table 1. Parameter values are not varied in any of the simulations presented here.

The model is made adimensional with respect to the length of the rectangular plate, L, the prescribed velocity U on the top boundary ~~,~~ and the undamaged elastic modulus E_0.

The system of equations is therefore given by Eq. (28) to (30) with $\frac{D\tilde{\mathbf{u}}}{D\tilde{t}} = 0$ and is solved for the 6 unknowns $\tilde{\mathbf{u}}$ (2 components), $\tilde{\sigma}$ (3 components) and d. In all simulations, the time step is set equal to the characteristic time for damage propagation ($\tilde{\Delta}t = T_d$). A semi-implicit scheme is used that linearizes the system, in which the momentum and constitutive equations are first solved simultaneously using a backward Euler scheme of ~~$O(1)$~~ order 1 and the value of ~~$\tilde{d}$~~ d at the previous model time step. The level of damage is updated in a second time using the estimated $\tilde{\mathbf{u}}$ and $\tilde{\sigma}$ and an explicit scheme of ~~$O(1)$.~~ order 1. A fixed-point algorithm iterates between these two steps until the residual of the linearized constitutive equation drops below a chosen tolerance, ensuring the convergence of the solution. Finite elements (FE) and variational methods are used to solve the time-discretized problem on a Lagrangian grid within the C++ environment RHEOLEF (Saramito, 2013: http://cel.archives-ouvertes.fr/cel-00573970). An unstructured mesh with triangular elements is used and the average spatial resolution is set by choosing the number N of elements along the short side of the domain.

~~All simulations are started from an initially undamaged ice cover with uniform elastic modulus and viscosity. Undamaged mechanical parameter values are chosen so that to be representative of sea ice on regional to global scales ($c = 500\,\mathrm{ms}^{-1}$ and $\nu = 0.3$). The undamaged elastic modulus is given by the relation $E^0 = 2c^2(1+\nu)\rho$ and the undamaged viscosity η^0 is set such that the initial relaxation time λ^0 is as large as possible while the maximum Weissenberg number, We^0 is small (<1). All model variables and parameters are listed in table 1. Parameter values are not varied in any of~~ As cumulative deformations are small (see above) the ~~experiments presented here as a sensitivity study is kept for a separate paper~~ FE spatial discretization is defined based on the initial mesh grid and is not updated in time. All results presented in the following are expressed in terms of adimensional quantities, however for the sake of simplicity we drop the '˜' notation for all variables.

7 Results

In this section we analyze the mechanical behaviour of the Maxwell-EB model. In particular, we evaluate its ~~capacity~~ capability to reproduce the main characteristics of sea ice deformation ~~, which~~
~~are its spatial -~~ its heterogeneity, intermittency and anisotropy ~~, following the methodology developed~~
~~in previous observational studies of the deformation and drift of the Arctic ice pack.~~

~~One signature of the strong heterogeneity of sea ice deformation is the emergence of a spatial~~
~~scaling in the deformation fields over a wide range of scales. Using a coarse-graining procedure,~~
~~performed a scaling analysis of the deformation of sea ice over the Arctic using the 3-days, 10 km × 10 km~~
~~gridded RGPS deformation product. Doing so, they obtained a power-law relationship between the~~
~~total deformation rate $< \dot\varepsilon_{tot} >_l$ invariant and the corresponding averaging scale l of the form~~

$$<_{tot} >_l \sim l^{-\beta}$$

~~with a constant exponent $\beta > 0$, indicating correlations in the deformation fields over 2 orders of~~
~~magnitude in l and an increase in the mean strain rate with decreasing scale of observation, in~~
~~agreement with a strong spatial localization of the deformation.~~

~~This coarse-graining calculation was later extended to ice buoy data which , with a higher temporal~~
~~resolution than the RGPS data, allowed performing scaling analyses of Arctic sea ice deformation~~
~~in the temporal dimension as well. Using the dispersion rate of buoys as a proxy for the strain rate,~~
~~obtained a power-law relationship between the total deformation rate $< \dot\varepsilon_{tot} >_t$ computed at a chosen~~
~~space scale and the time scale of observation t~~

$$<_{tot} >_t \sim t^{-\gamma}$$

~~with a constant exponent $\gamma > 0$ over 2 orders of magnitudes in t (3 hours to 3 months), indicating an~~
~~increase of strain rates with decreasing temporal scale consistent with an intermittent deformation~~
~~process. Recently, these temporal and spatial scaling properties have been -~~ which have been recently
used as benchmarks to validate (or invalidate) sea ice models (e.g., Girard et al., 2009, 2010; Bouillon
and Rampal, 2015).

~~An additional and all-important characteristic~~ To do so, we follow the methodology developed in
previous observational studies of the deformation ~~of sea ice that is not captured by these scaling~~
~~analyses is its strong anisotropy. This property has been made evident since the availability of~~
~~satellite imagery-derived ice motion products , which showed that high strain rates concentrate along~~
~~oriented, linear-like faults, or leads, often termed "linear kinematic features"~~ and drift of the Arctic
ice pack.

7.1 Spatial resolution, convergence and ~~dependence on the initial conditions~~anisotropy

In a first time, we analyze the overall, macroscopic behaviour of the Maxwell-EB model ~~, its~~
~~convergence properties and the dependance~~ as well as the convergence and dependence of the so-

22

lution on the prescribed initial conditions. To do so, a set of four uniaxial compression simulations is run using different spatial resolutions, with $N = 10$, 20, 40 and 80. The values of the initial, undamaged mechanical parameters are identical between the simulations~~as well as~~. So is the field of cohesion, which is defined at the lowest resolution ($N = 10$) and interpolated onto the higher resolution mesh grids.

Figure 5 shows the (adimensional) macroscopic stress, σ_m (normal stress integrated on the upper boundary of the domain), as a function of the ~~adimensional~~ (adimensional) macroscopic strain, ε_m, set by the prescribed displacement of the upper boundary, for these four simulations. The dotted line represents the damage rate (the number of damaged elements per model time step times their distance to the damage criterion, $1 - d_{crit}$) for the simulation with $N = 40$. Inspection of the initial loading and damaging sequence suggests that the mechanical behaviour is similar to that obtained with other elasto-brittle models (e.g., Tang, 1997; Amitrano et al., 1999; Girard et al., 2010). The Maxwell-EB model simulates

1. a strictly linear-elastic behaviour at the initial stage of the experiment, as the material is initially undamaged,

2. a deviation from the linear-elastic behaviour after the onset of damage (marked by the red dot 1), indicative of macroscopic strain softening, with damage distributed homogeneously throughout the material (see Fig. 5 b1),

3. the formation of clusters of damaged elements, non-interacting at first, then joining along linear features. This stage is marked by a rapid increase in the number of damaged elements,

4. a sharp stress drop associated with the macroscopic failure of the sample and propagation of a main fault spanning the entire domain (see Fig. 5 b2).

In the Maxwell-EB model, this last stage is characterized by a drop in the Weissenberg number (i.e., in λ) localized along the main fault (not shown), where strain rates are orders of magnitude higher than ~~over~~ in undamaged parts of the material. Then, as damaged areas heal, stress builds up again within the material. At all spatial resolutions, the model simulates cycles of slow stress build ups (healing phase) and rapid stress relaxations (damaging phase).

Because the simulations use the same spatial distribution of the damage ~~criteria~~ threshold (i.e., of C) the location of the first damage events is the same at all resolutions, as shown by the maps of instantaneous level of damage d near the onset of damaging (Fig. 5 b1). ~~However, soon after these first failure events , model solutions~~ As soon as the first damage events occur, the heterogeneities introduced in the stress field by these events contribute and, over time, prevail over the initially introduced noise in C in setting the location and timing of subsequent events (Tang, 1997). Because these heterogeneities tend to localize at the finest scale (i.e., the scale of the mesh element, Δx), their generation results in a different redistribution of the stress between neighbouring elements and

23

hence in a non-identical propagation of damage between the model simulations at different spatial resolutions. As illustrated on figure 5, the model solutions therefore do not converge (~~Fig. 5 b2-4~~see panels b, 2 to 4) and fractures form with ~~a shape and orientation differing between simulations.~~ different shapes and orientations.

745   This divergence between the post-damage model solutions illustrates an all-important and intrinsic characteristic of the ~~Maxwell-EB framework arising from the fact that~~ present rheological framework. As other models for the failure of disordered materials (e.g., Cowie et al., 1993; Tang, 1997; Amitrano et al., 1999; Girard et al., 2011), the Maxwell-EB model is based on the standard formulation of damage theory, in which there is no ~~physical~~ characteristic length scale associated

750 with ~~the localization of damage in the model. Through elastic interactions, damage and deformation tend to localize at the finest scale (the mesh element) , resulting in a different redistribution of~~ damage redistribution and damage is therefore *local*. One instrinsic property of this local damage theory is that it allows damage to localize into a zone of vanishing volume (or area) (Bažant, 1976), thereby implying a zero energy dissipation rate in that volume (area). As a consequence, the numerical

755 solutions of finite element local damage models are not objective with respect to the choice of mesh grid and do not converge upon mesh refinement.

    These shortcomings have been dealt with by defining damage in models in a non-local manner (see Bažant and Jirásek (2002) for a review of such models). Pijaudier-Cabot and Bažant (1987) for instance have suggested applying the non-local concept to the variables controlling the strain

760 softening, i.e., the level of damage, while keeping a local definition for the elastic strain and stresses in the ~~stress between neighbouring elements at different spatial resolutions and hence a non-identical propagation of the damage. Put another way, the divergence of the solutions indicates that while the disorder in *C* sets the location of the first damage events, the heterogeneities introduced in the stress field by these events prevail in setting the location and timing of subsequent events. This result is~~

765 ~~consistent with previous elasto-brittle model simulations which have shown that the number of active faults as well as the degree of localization of the deformation over long time scales do not depend systematically on the disorder initially introduced in the model and that once formed, faults produce their own stress field which dominates further fracture growth~~ linear-elastic constitutive equation. By replacing the damage energy release rate with its spatial average over a representative volume

770 (area), the localization of damage is then limited to a space scale that corresponds to an intrinsic damage length scale for the simulated material. In the context of sea ice, following this approach would entail assuming a minimum size for leads within the ice pack, or a correlation length, $\xi > \Delta x$ for heterogeneities within the ice cover. Such assumption would however not be physical, as the correlation length associated with natural heterogeneities (see section 4.2) is likely much smaller

775 than that of the grid cell in regional and global sea ice models. In addition, invariance of sea ice fracturing, as revealed from floe sizes distributions, holds down to the meter scale (e.g. Weiss, 2003).

Another important property of the deformation made evident by this set of experiments is its strong anisotropy. The fields of d and of the total deformation rate ($\dot{\varepsilon}_{tot}$) represented on Fig. 5 indeed show that at all spatial resolutions, the simulated damage and deformation are both highly
780 localized and oriented along linear features. This is an important result, as no anisotropy is introduced at the local scale on either the elastic or viscous properties, or in the damage parameterization. ~~This property arises naturally due to elastic interactions within the material and without the need to prescribe fault orientations. It was reproduced by the original EB model and is not lost when including a viscous dissipation term for the stress in~~ In an elastic medium submitted to a loading that
785 is non-perfectly isotropic with respect to the domain geometry or the heterogeneity present in the material, the elastic kernel associated with a damaged inclusion is indeed anisotropic, hence is the redistribution of stresses (Eshelby, 1957). This is illustrated in Fig. 6(a), which shows the field of the Coulomb stress, $\sigma_{Coulomb} = \sigma_1 - q\sigma_2$ (i.e., the maximum stress with respect to the ~~Maxwell-EB constitutive relationship~~Mohr-Coulomb damage criterion, right panel) associated with the presence
790 of a circular damaged inclusion in an otherwise homogeneous, isotropic, linear-elastic rectangular plate subjected to the same uniaxial compression loading and boundary conditions as described in section 6. In the simulations presented here each element, as soon as it becomes damaged, plays the role of a damaged inclusion and induces a long-range perturbation in the stress field that is maximum along oriented branches (see Fig. 6b). The combination of (1) small-scale disorder, (2)
795 damage mechanics in an elastic medium and (3) the anisotropy of the elastic interaction kernel itself is sufficient to generate anisotropy, up to very large space scales through successive elastic interactions between damaged elements.

7.2 Heterogeneity

As shown in the previous section, when simulations are started from an undamaged state, the simu-
800 lated mechanical behaviour of the material is intrinsically different between the first and subsequent loading and damaging cycles. The ~~path to the first rupture in "irreversible damage " (i.e., models without healing) elasto-brittle~~ capability of damage models based on a linear-elastic constitutive law to reproduce a deformation that is highly heterogeneous has already been ~~investigated in depth~~ demonstrated (e.g. Girard et al., 2010; Tang, 1997; Amitrano et al., 1999). ~~Hence~~However, as these
805 frameworks neither include a healing mechanism nor a slow relaxation of elastic stresses, their post-macroscopic failure behaviour is physically inconsistent, and only the path to the first rupture was analyzed. Hence here we focus our analysis ~~of the spatial dependence of the Maxwell-EB model strain rate fields~~ on the ~~post macro-rupture behaviour.~~ post-macroscopic rupture behaviour and aim to establish if the strain-rate fields simulated with the Maxwell-EB model model exhibit a similar
810 heterogeneity.

To quantify the ~~heterogeneity~~ spatial localization of the simulated deformation, we follow Marsan et al. (2004) and estimate deformation rates over two orders of magnitude in space scales using a

coarse-graining procedure. The calculation is described in details by Girard et al. (2010). For this analysis we use ~~the~~ outputs of strain rate fields from simulations with $N = 100$, averaged over a
815   time interval corresponding to the time of propagation of an elastic shear wave with speed c through the width of the domain ($\frac{L}{2}\frac{1}{T \times c} = N$ time steps). The dependence of the deformation rates on the spatial scale of observation is investigated at different stages of the healing-damaging cycle. Figure 7 (a and b) shows the total deformation rate $< \dot{\varepsilon}_{tot} >_l$ as a function of the space scale l at 5 equally-spaced steps along the path towards a given macroscopic failure event, that is, between the minimum
820   in macroscopic stress that follows the propagation of a fault and the maximum that precedes the next macro-rupture, as indicated in Fig. 7(a). Deformation rates are normalized by $< \dot{\varepsilon}_{tot} >$ at the smallest averaging scale (L/N). At the first stage, just following the rupture (red curve), the total deformation rate shows a clear power law decrease with increasing spatial scale of the form of Eq. (1) over nearly two orders of magnitude of l, consistent with a strong localization of the deformation.
825   At the subsequent stages (yellow and green curves), damaged elements progressively recover their mechanical strength by healing. Deformation rates decrease along the main fault and re-increases over undamaged areas, hence deformation homogenizes over the domain and the rate of decrease of $< \dot{\varepsilon}_{tot} >_l$ with l is reduced. Then, as healing allows stress to build up within the material, damaging resumes and ~~clusters in space and the~~ localizes again. The exponent β therefore re-increases towards
830   its post macro-rupture value (blue and purple curves).

    Repeating the procedure for subsequent healing and damaging cycles and for multiple realizations of the experiment initialized with different cohesion fields showed a similar evolution of the rate of decrease of $< \dot{\varepsilon}_{tot} >_l$ with l between macro-ruptures events, with values of β in the vicinity of the rupture consistent with previous EB model analyses (e.g., Girard et al., 2010, $\beta = 0.15 \pm 0.02$).
835   However, an important difference between the present results and that of Girard et al. (2010) is the absence of a clear cross-over scale for which $< \dot{\varepsilon}_{tot} >_l$ becomes independent of l and which implies a finite correlation length of damage events. This suggests that the Maxwell-EB system progressively looses the memory of ~~it's~~ its initial homogeneous, undamaged state and that an elasto-brittle material experiencing both healing and damaging enters a "marginally stable" state with scale invariance
840   spanning the size of the system. This result is consistent with the scale-dependence analysis of RGPS-derived deformation rates of Marsan et al. (2004) and Stern and Lindsay (2009), in which no cutoff scale was observed for l varying between 10 and 1000 km, suggesting that Arctic sea ice is most often in a near-critical state.

7.3   Intermittency

845   In this section we characterize the temporal behaviour of the Maxwell-EB model. Figure 8(a) represents the simulated macroscopic stress as a function of time (black dashed-dotted line) along with the corresponding damage rate (grey solid line) record for one realization of the uniaxial compres-

sion experiment with $N = 40$. Inspection of both temporal series reveals two types of mechanical behaviour of the Maxwell-EB material.

850   First, the evolution of the macroscopic stress is clearly characterized by cycles of slow stress build-ups and very fast relaxations. The strong asymmetry of the signal in time is confirmed by a high (negative) skewness (-6) of the distribution of the macroscopic stress increments $\frac{\Delta \sigma_m}{\Delta t}$ (not shown). Associated with these cycles is a succession of progressive increases in damage events and very sharp drops, after which damaging stops momentarily (red arrow on Fig. 8a).

855   Second, as identified on the same time series, some periods (e.g., the interval delimited by the dashed red box) are characterized by a continuous damage activity and by both low amplitude and low frequency fluctuations of the stress. This contrasted behaviour translates into a significantly more symmetric (skewness of -1.9) distribution of $\frac{\Delta \sigma_m}{\Delta t}$. Inspection of the spatial distribution of damage (Fig. 8b) and strain rate fields (not shown) over this time interval indicates that the same system of

860   interacting faults remains activated, with not much damaging activity over the rest of the domain and therefore suggests that creep-like deformation along this system dissipates all of the input loading.

Following the approach taken for fracture-type models which record the number of broken fibres, ruptured bounds, depinning events, etc., we investigate the time-dependence of the simulated damage activity by analyzing time series of ~~the~~ discrete failure events. We estimate the power spectral density

865   (PSD) of damage rate time series. The resulting squared Fourier coefficients are averaged over 5 realizations of the compression experiment initialized with different fields of C over domains with $N = 40$. Fig. 9(a) represents the spectral density estimated by averaging the power over a 5 values window centred on each frequency f. We checked that using a smaller averaging window does not affect the shape of the PSD discussed below.

870   At low frequencies, the PSD is almost flat, suggesting that the number of damage events is un-correlated in time. As these frequencies are lower than $\frac{1}{T_h}$, this is consistent with the fact that the Maxwell-EB material entirely looses the memory of previous damage events when allowed to heal completely. At higher frequencies, the PSD shows a decrease with increasing f reminiscent of a temporal correlation of damaging events in the material. This expresses as a power law decay with

875    $\mathrm{PSD}(f) = 1/f^\gamma$. At intermediate frequencies, we estimate a slope $\gamma = 2$, suggesting that the instantaneous damage rate is correlated in time but *increments* of the damage rate are uncorrelated. At the highest frequencies, $\gamma > 2$, indicating that the damage rate is correlated in time and ~~the of damage rate~~ damage rate increments are anti-correlated. The break in the slope occurs around $f = 10^6$, a frequency that we relate to the minimum propagation time of a macro-rupture, i.e., the time of prop-

880   agation of damage (i.e., of an elastic shear wave with speed c) across the width $\frac{L}{2}$ of the domain (N time steps). The transition between the flat and power law decaying parts of the PSD is marked by a clear peak spanning the range of frequencies corresponding to the cycles of healing and damaging, the ~~red~~ dashed line indicating the frequency of such a cycle, as identified by the double arrow on Fig. 8(a).

885　Finally, we analyze the ~~dependance~~ dependence of the simulated deformation on the time scale of observation using a temporal coarse-graining method (e.g., Rampal et al., 2008). Components of the strain rate at a given spatial scale are averaged over a time window of duration t to compute the mean total deformation rate $< \dot{\varepsilon}_{tot} >_t$. The window is centred on an arbitrary time t_0 and has a size $t = 2n \times (N\Delta t)$ with $n = 1, 2, 3, ...$ and with the smallest averaging time scale corresponding to the

890　time of propagation of an elastic shear wave with speed c across the width $\frac{L}{2}$ of the domain. The chosen spatial averaging scale is that of the highest deformation rate, which as shown in section 1 is of $\frac{L}{N}$. The domain is therefore divided in square boxes of equal size $l = \frac{L}{N}$ and the calculated deformation invariants are averaged over all available boxes. Figure 9(b) shows the total deformation rate $< \dot{\varepsilon}_{tot} >_t$ as a function of the time of observation t (thick black line) averaged over 20 realizations

895　of the coarse graining calculation (thin ~~, coloured~~ grey lines) centred on different t_0 for a simulation with $N = 40$. Consistent with the localizing of the deformation and an intermittent process, $< \dot{\varepsilon}_{tot} >_t$ decreases with increasing t over almost two orders of magnitudes of t.

The observed scaling is however altered in two ways, which relate to the specific geometry, loading and boundary conditions used in the present simulations. First, as one main fault always dom-

900　inates the deformation in the system, curves of $< \dot{\varepsilon}_{tot} >_t$ are strongly modulated by a succession of peaks associated with the cycles of stress build-up and macro-rupture, the amplitude of which decreases with the scale of observation t. Second, at large t, the scaling ~~assymptotes~~ asymptotes to a value corresponding to the prescribed forcing. Simulations over larger systems using non-homogeneous surface forcing should allow for multiple macroscopic scale faults to be active si-

905　multaneously and hence to observe a clearer scaling of the simulated deformation over larger time spans.

8　Conclusions

In this paper we have presented a new mechanical framework suited for modelling the brittle behaviour of the sea ice cover (Weiss et al., 2007) while keeping a continuum description. A relaxation

910　term for the internal stress is added to the original Elasto-Brittle constitutive ~~relationship~~ law and both the linear and viscous components are coupled to a progressive damage mechanism to allow partitioning between the reversible and permanent deformations ~~within the material based on its~~ based on the local level of damage of the material.

Highly idealized simulations using forcing conditions homogeneous in both space and time show

915　the Maxwell-EB model simulates a complex temporal and spatial evolution of the deformation patterns, in close agreement with observations of the Arctic sea ice cover. Anisotropy in the simulated damage and deformation fields arises naturally from the small-scale disorder and elastic interactions, although the material's properties are fully isotropic at the element scale. The model also reproduces both the persistence of creeping leads and the activation of new leads with different shapes and ori-

920 entations, in agreement with the observed deformation of sea ice (Coon et al., 2007). Analyses of the simulated damage and deformation fields reveal

1. a highly heterogeneous deformation, translating into a power law decrease of the deformation rate with increasing spatial scale. The associated exponent varies periodically: it is highest in the vicinity of macro-rupture events and decreases between events as the material partially

925 heals. The disappearance after a few "spinup" rupture events of a cross-over scale at which deformation rates become independent of the scale of observation suggests that the Maxwell-EB model, including both damaging and healing processes, successfully reproduces a "marginally stable" state, as observed for Arctic sea ice.

2. an intermittent deformation, manifested by the highly asymmetric temporal evolution of the

930 internal stress within the material, which shows a succession of slow build-ups and very rapid relaxation phases. This intermittency is supported by the existence of a temporal correlation in the rate of damage at all timescales below the ~~material's~~ characteristic healing time of the material. A temporal scaling of the deformation rate is also obtained but due to the specific setup of the simulations analyzed here, it is modulated by the cycles of stress build-up and

935 relaxation and its span is limited by the prescribed forcing.

Considering the highly idealized setup of the simulations analyzed here, these temporal and spatial scaling properties in the deformation fields cannot possibly be inherited from the prescribed forcing. Instead, their emergence is a signature of the mechanical behaviour of the Maxwell-EB model itself.

The next logical step in the development of a Maxwell-EB sea ice rheology consists in analyzing

940 the sensitivity of the simulated deformation and damage fields to the model parameters. In particular, the partitioning between the simulated brittle and creep-like behaviour as well as the degree of localization of the deformation (Frederiksen and Braun, 2001) might depend on the rate of decrease of the viscous relaxation time with increasing level of damage (parameter α) and on the characteristic time for healing and associated healing parameterization, all of which are poorly constrained in the

945 case of the ice pack.

Further validation of the Maxwell-EB framework and the determination of the range of model parameters values suitable for sea ice call for a thorough comparison of the scaling properties of the simulated deformation rates with that estimated from the available ice buoy and RGPS data. Such analysis necessitates carrying out numerical experiments over periods of several days to months and

950 over realistic domains of regional to global scales. At these spatial and temporal scales, deformations within the sea ice cover become large. Hence advective processes cannot be neglected. As the Maxwell-EB rheology effectively reproduces very strong spatial gradients within the velocity, strain and stress fields, its use in large-deformation experiments requires the implementation of a robust advection scheme in order to limit diffusion and retain the strong localization of damage and defor-

955 mation rates. The development of a numerical scheme for the ~~the~~ Maxwell-EB model that includes

29

advection and is both efficient and practical in view of dynamic-thermodynamic and fully coupled ocean-sea ice-atmosphere simulations is underway.

References

965   Agnon, A. and Lyakhovsky, V.: Damage distribution and localization during dyke intrusion, pp. 65–78, A. A. Balkema, Brookfield, Vt, 1995.

Amitrano, D., Grasso, J.-R., and Hantz, D.: From diffuse to localised damage through elastic interaction, Geophysical Research Letters, 26, 2109–2112, 1999.

Aranson, I. S. and Tsimring, L. S.: Patterns and collective behavior in granular media: Theoretical concepts, Rev.

970   Mod. Phys., 78, 641–692, doi:10.1103/RevModPhys.78.641, http://link.aps.org/doi/10.1103/RevModPhys.78.641, 2006.

Bažant, Z. P.: Instability ductility and size effect in strain-softening concrete, Journal of Engineering Mechanics Division, 102, 331–344, 1976.

Bažant, Z. P. and Jirásek, M.: Nonlocal Integral Formulations of Plasticity and Damage: Survey of Progress,

975   Journal of Engineering Mechanics, 128, 1119–1149, doi:10.1061/(ASCE)0733-9399(2002)128:11(1119), http://dx.doi.org/10.1061/(ASCE)0733-9399(2002)128:11(1119), 2002.

Borstad, C. P., Khazendar, A., Larour, E., Morlighem, M., Rignot, E., Schodlok, M. P., and Seroussi, H.: A damage mechanics assessment of the Larsen B ice shelf prior to collapse: Toward a physically-based calving law, Geophysical Research Letters, 39, doi:10.1029/2012GL053317, l18502, 2012.

980   Bouillon, S. and Rampal, P.: Presentation of the dynamical core of neXtSIM a new sea ice model, Ocean Modelling, 91, 23–37, doi:http://dx.doi.org/10.1016/j.ocemod.2015.04.005, 2015.

Byerlee, J.: Friction of rocks, Pure and Applied Geophysics, 116, 615–626, doi:10.1007/BF00876528, 1978.

Cakir, Z., Ergintav, S., Ozener, H., Dogan, U., Akoglu, A. M., Meghraoui, M., and Reilinger, R.: Onset of aseismic creep on major strike-slip faults, Geology, 40, 1115–1118, doi:10.1130/G33522.1, 2012.

985   Cetin, E., Cakir, Z., Meghraoui, M., Ergintav, S., and Akoglu, A. M.: Extent and distribution of aseismic slip on the Ismetpa?a segment of the North Anatolian Fault (Turkey) from Persistent Scatterer InSAR, Geochemistry, Geophysics, Geosystems, 15, 2883–2894, doi:10.1002/2014GC005307, http://dx.doi.org/10.1002/2014GC005307, 2014.

Coon, M., Kwok, R., Levy, G., Puis, M., Schreyer, H., and Sulsky, D.: Arctic Ice Dynamics Joint Ex-

990   periment (AIDJEX) assumptions revisited and found inadequate, Journal of Geophysical Research, 112, doi:10.1029/2005JC003393, 2007.

Cowie, P. A., Vanneste, C., and Sornette, D.: Statistical Physics Model for the Spatiotemporal evolution of faults, Journal of Geophysical Research, 98, 21 809–21 821, 1993.

Cowie, P. A., Sornette, D., and Vanneste, C.: Multifractal scaling properties of a growing fault population,

995   Geophysical Journal International, 122, 457–469, 1995.

Duval, P., Ashby, M. F., and Anderman, I.: Rate-controlling processes in the creep of polycrystalline ice, The Journal of Physical Chemistry, 87, 4066–4074, doi:10.1021/j100244a014, 1983.

Eshelby, J. D.: The Determination of the Elastic Field of an Ellipsoidal Inclusion, and Related Problems, Proceedings of the Royal Society of London A: Mathematical, Physical and Engineering Sciences, 241, 376–

1000   396, doi:10.1098/rspa.1957.0133, 1957.

Fattal, R. and Kupferman, R.: Constitutive laws for the matrix-logarithm of the conformation tensor, Journal of Non-Newtonian Fluid Mechanics, 123, 281–285, 2004.

Fattal, R. and Kupferman, R.: Time-dependent simulation of viscoelastic flows at high Weissenberg number using the log-conformation representation, Journal of Non-Newtonian Fluid Mechanics, 126, 23–37, 2005.

1005 Flato, G., Marotzke, J., Abiodun, B., Braconnot, P., Chou, S. C., Collins, W., Cox, P., Driouech, F., Emori, S., Eyring, V., Forest, C., Gleckler, P., Guilyardi, E., Jakob, C., Kattsov, V., C., R., and Rummukainen, M.: Climate Change 2013: The Physical Science Basis. Contribution of Working Group I to the Fifth Assessment Report of the Intergovernmental Panel on Climate Change, chap. Evaluation of Climate Models, p. 126 pp., Cambridge University Press, Cambridge, United Kingdom and New York, NY, USA, 2013.

1010 Fortt, A. L. and Schulson, E. M.: The resistance to sliding along Coulombic shear faaults in ice, Acta Materialia, 55, 2253–2264, 2007.

Frederiksen, S. and Braun, J.: Numerical modelling of strain localisation during extension of the continental lithosphere, Earth and Planetary Science Letters, 188, 241–251, 2001.

Girard, L., Weiss, J., Molines, J. M., Barnier, B., and Bouillon, S.: Evaluation of high-resolution sea ice models 1015 on the basis of statistical and scaling properties of Arctic sea ice drift and deformation, Journal of Geophysical Research, 114, doi:10.1029/2008JC005182, 2009.

Girard, L., Amitrano, D., and Weiss, J.: Failure as a critical phenomenon in a progressive damage model, Journal of Statistical Mechanics : Theory and Experiment, P01013, doi:10.1088/1742-5468/2010/01/P01013, 2010.

Girard, L., Bouillon, S., Weiss, J., Amitrano, D., Fichefet, T., and Legat, V.: A new modeling framework for sea 1020 ice models based on elasto-brittle rheology, Annals of Glaciology, 52, 2011.

Gratier, J. P., Renard, F., and Vial, B.: Postseismic pressure solution creep: Evidence and time-dependent change from dynamic indenting experiments, Journal of Geophysical Research: Solid Earth, 119, 2764–2779, doi:10.1002/2013JB010768, 2014.

Hamiel, Y., Liu, Y., Lyakhovsky, V., Ben-Zion, Y., and Lockner, D.: A viscoelastic damage model 1025 with applications to stable and unstable fracturing, Geophysical Journal International, 159, 1155–1165, doi:10.1111/j.1365-246X.2004.02452.x, 2004.

Herrmann, H. J. and Roux, S., eds.: Statistical Models for the fracture of disordered meria, North-Holland, Amsterdam, 1990.

Hibler, W. D. I.: A viscous sea ice law as a stochastic average of plasticity, Journal of Geophysical Research, 1030 82, 3932–3938, 1977.

Hibler, W. D. I.: A dynamic thermodynamic sea ice model, Journal of Physical Oceanography, 9, 815–846, 1979.

Hibler, W. I.: Sea ice fracturing on the large scale, Engineering Fracture Mechanics, 68, 2013 – 2043, doi:http://dx.doi.org/10.1016/S0013-7944(01)00035-2, 2001.

1035 Hutchings, J. K., Roberts, A., Geiger, C. A., and Richter-Menge, J.: Spatial and temporal characterization of sea-ice deformation, Annals of Glaciology, 52, 360–368, 2011.

Jaeger, J. C. and Cook, N. G. W.: Fundamentals of Rock Mechanics, Chapman and Hall, Cambridge UK, 1979.

Jop, P., Forterre, Y., and Pouliquen, O.: A constitutive law for dense granular flows, Nature, 441, 727–230, doi:10.1038/nature04801, 2006.

1040 Kagan, Y.: Fractal dimension of brittle fracture, Journal of Nonlinear Science, 1, 1–16, doi:10.1007/BF01209146, 1991.

Kagan, Y. Y. and Jackson, D. D.: Long-Term Earthquake Clustering, Geophysical Journal International, 104, 117–134, doi:10.1111/j.1365-246X.1991.tb02498.x, 1991.

Kagan, Y. Y. and Knopoff, L.: Spatial distribution of earthquakes: the two-point correlation function, Geophysical Journal International, 62, 303–320, doi:10.1111/j.1365-246X.1980.tb04857.x, 1980.

Keller, A. and Hutter, K.: A viscoelastic damage model for polycrystalline ice, inspired by Weibull-distributed fiber bundle models. Part I: Constitutive models, Continuum Mechanics and Thermodynamics, 26, 879–894, doi:10.1007/s00161-014-0348-7, http://dx.doi.org/10.1007/s00161-014-0348-7, 2014.

Keunings, R.: On the high Weissenberg number problem, Journal of Non-Newtonian Fluid Mechanics, 20, 209–226, 1986.

King, G. C. P., Stein, R. S., and Lin, J.: Static stress change and the triggering of earthquakes, Bulletin of the Seismological Society of America, 84, 935–953, 1994.

Krug, J., Weiss, J., Gagliardini, O., and Durand, G.: Combining damage and fracture mechanics to model calving, The Cryosphere, 8, 2101–2117, doi:10.5194/tc-8-2101-2014, http://www.the-cryosphere.net/8/2101/2014/, 2014.

Kwok, R.: Deformation of the Arctic Ocean sea ice cover: November 1996 through April 1997, in: IUTAM Symposium on Scaling Laws in Ice Mechanics and Ice Dynamics, edited by Dempsey, J. and Shen, H. H., Solid Mechanics and Its Applications, pp. 315–323, Springer Netherlands, doi:10.1007/978-94-015-9735-7, 2001.

Kwok, R., Hunke, E. C., Maslowski, W., Menemenlis, D., and Zhang, J.: Variability of sea ice simulations assessed with RGPS kinematics, Journal of Geophysical Research: Oceans, 113, doi:10.1029/2008JC004783, http://dx.doi.org/10.1029/2008JC004783, c11012, 2008.

Lindsay, R. W., Zhang, J., and Rothrock, D. A.: Sea-ice deformation rates from satellite measurements and in a model, Atmosphere-Ocean, 41, 35–47, doi:10.3137/ao.410103, 2003.

Lyakhovsky, V., Ben-Zion, Y., and Agnon, A.: Distributed damage, faulting and friction, Journal of Geophysical Research, 102, 27 635–27 649, 1997.

Marsan, D. and Weiss, J.: Space/time coupling in brittle deformation at geophysical scales, Earth and Planetary Science Letters, 296, 353–359, 2010.

Marsan, D., Stern, H., Lindsay, R., and Weiss, J.: Scale dependance and localization of the deformation of Arctic sea ice, Physical Review Letters, 93, doi:10.1103/PhysRevLett.93.178501, 2004.

Marsan, D., Weiss, J., Metaxian, J.-P., Grangeon, J., Roux, P.-F., and Haapala, J.: Low frequency bursts of horizontally-polarized waves in the Arctic sea-ice cover, Journal of Glaciology, 57, 231–237, 2011.

Maxwell, J. C.: On the dynamical theory of gases, Philosophical Transactions of the Royal Society of London, 157, 49–88, 1867.

Maykut, G. A.: The surface heat and mass balance, pp. 395–463, NATO ASI series, Series B: Physics, Springer US, doi:10.1007/978-1-4899-5352-0_6, 1986.

Nye, J. F.: Is there any physical basis for assuming linear viscous behavior for sea ice?, Aidjex Bulletin, 6, 18–19, 1973.

Paul, B.: A modification of the Coulomb-Mohr theory of fracture, Journal of Applied Mechanics, 28, 259–268, 1961.

Petrich, C., Langhorne, P., and Haskell, T.: Formation and structure of refrozen cracks in land-fast first-year sea ice, Journal of Geophysical Research, 112, C04,006, doi:10.1029/2006JC003466, 2007.

Pijaudier-Cabot, G. and Bažant, Z. P.: Nonlocal damage theory, Journal of Engineering Mechanics, 113, 1512–1533, 1987.

Pralong, A. and Funk, M.: Dynamic damage model of crevasse opening and application to glacier calving, Journal of Geophysical Research: Solid Earth, 110, doi:10.1029/2004JB003104, http://dx.doi.org/10.1029/2004JB003104, b01309, 2005.

Rampal, P., Weiss, J., Marsan, D., Lindsay, R., and Stern, H.: Scaling properties of sea ice deformation from buoy dispersion analysis, Journal of Geophysical Research: Oceans, 113, n/a–n/a, doi:10.1029/2007JC004143, http://dx.doi.org/10.1029/2007JC004143, c03002, 2008.

Rampal, P., Weiss, J., Marsan, D., and Bourgoin, M.: Arctic sea ice velocity field: General circulation and turbulent-like fluctuations, Journal of Geophysical Research: Oceans, 114, n/a–n/a, doi:10.1029/2008JC005227, http://dx.doi.org/10.1029/2008JC005227, c10014, 2009.

Rothrock, D. A.: The energetics of the plastic deformation of pack ice by ridging, Journal of Geophysical Research, 80, 4514–4519, 1975.

Sakov, P., Counillon, F., Bertino, L., Lisaeter, K. A., Oke, P. R., and Korablev, A.: TOPAZ4: An ocean-sea ice data assimilation system for the North Atlantic and Arctic, Ocean Sciences, 8, 633–656, doi:10.5194/os-8-633-2012, 2012.

Saramito, P.: On a modified non-singular log-conformation formulation for Johnson-Segalman viscoelastic fluids, Journal of Non-Newtonian Fluid Mechanics, 211, 16–30, 2014.

Saramito, P.: Complex fluids. Modelling and algorithms, To appear - Springer, 2016.

Schapery, R. A.: Nonlinear viscoelastic and viscoplastic constitutive equations with growing damage, International Journal of Fracture, 97, 33–66, 1999.

Scholz, C. H.: The Mechanics of Earthquakes and Faulting, Cambridge University Press, New York, 2 edn., 2002.

Schreyer, H. L., Sulsky, D. L., Munday, L. B., Coon, M. D., and Kwok, R.: Elastic-decohesive constitutive model for sea ice, Journal of Geophysical Research, 111, doi:10.1029/2005JC003334, 2006.

Schulson, E., Fortt, A., Iliescu, D., and Renshaw, C.: On the role of frictional sliding in the compressive fracture of ice and granite: Terminal vs. post-terminal failure, Acta Materialia, 54, 3923 – 3932, doi:10.1016/j.actamat.2006.04.024, 2006b.

Schulson, E. M.: Compressive shear faults within arctic sea ice: Fractures on scales large and small, Journal of Geophysical Research, 109, doi:10.1029/2003JC002108, 2004.

Schulson, E. M.: Failure envelope of first-year Arctic sea ice: The role of friction in compressive fracture, Journal of Geophysical Research, 111, doi:10.1029/2005JC003235, 2006a.

Schulson, E. M. and Duval, P.: Creep and Fracture of Ice, Cambridge University Press, Cambridge, UK, 2009.

Smith, G. C., Roy, F., Rezka, M., Surcel, M., Colan, D., Deacu, Z. He, D., Bélanger, J.-M., Skachko, S., Liu, Y., Dupont, F., Lemieux, J.-F., Beaudoin, C., Tranchant, B., Drévillon, M., Garric, G., Testut, C.-E., Lellouche, J.-M., Pellerin, P., Ritchie, H., Lu, Y., Davidson, F., Buehner, M., Caya, A., and Lajoie, M.: Sea ice forecast verification in the Canadian Global Ice Ocean Prediction System, Quarterly Journal of the Royal Meteorological Society, doi:10.1002/qj.2555, 2015.

Stein, R. S.: The role of stress transfer in earthquake occurrence, Nature, 402, 605–609, doi:10.1038/45144, 1999.

Stern, H. L. and Lindsay, R. W.: Spatial scaling of Arctic sea ice deformation, Journal of Geophysical Research, 114, doi:10.1029/2009JC005380, 2009.

1125   Stern, H. L., Rothrock, D. A., and Kwok, R.: Open water production in arctic sea ice: Satellite measurements and model parameterizations, Journal of Geophysical Research, 100, 20 601–20 612, 1995.

Tang, C.: Numerical Simulation of Progressive Rock Failure and Associated Seismicity, International Journal of Rock Mechanics and Mining Sciences, 34, 249–261, 1997.

Timco, G. and Weeks, W.: A review of the engineering properties of sea ice, Cold Regions Science and Tech-

1130   nology, 60, 107 – 129, doi:http://dx.doi.org/10.1016/j.coldregions.2009.10.003, 2010.

Tsamados, M., Feltham, D. L., and Wilchinsky, A. V.: Impact of a new anisotropic rheology on simulations of Arctic sea ice, Journal of Geophysical Research: Oceans, 118, 91–107, doi:10.1029/2012JC007990, 2013.

Turcotte, D. L.: Fractals and Chaos in geology and geophysics, Cambridge University Press, New York, 1992.

Weiss, J.: Scaling of Fracture and Faulting of Ice on Earth, Surveys in Geophysics, 24, 185–227,

1135   doi:10.1023/A:1023293117309, http://dx.doi.org/10.1023/A:1023293117309, 2003.

Weiss, J. and Schulson, E. M.: Coulombic faulting from the grain scale to the geophysical scale: lessons from ice, Journal of Physics D: Applied Physics, 42, 214 017, 2009.

Weiss, J., Schulson, E. M., and Stern, H. L.: Sea ice rheology from in-situ, satellite and laboratory observations: Fracture and friction, Earth and Planetary Science Letters, 255, 1–8, 2007.

1140   Wilchinsky, A. V. and Feltham, D. L.: Modelling the rheology of sea ice as a collection of diamond-shaped floes, Journal of Non-Newtonian Fluid Mechanics, 138, 22–32, 2006.
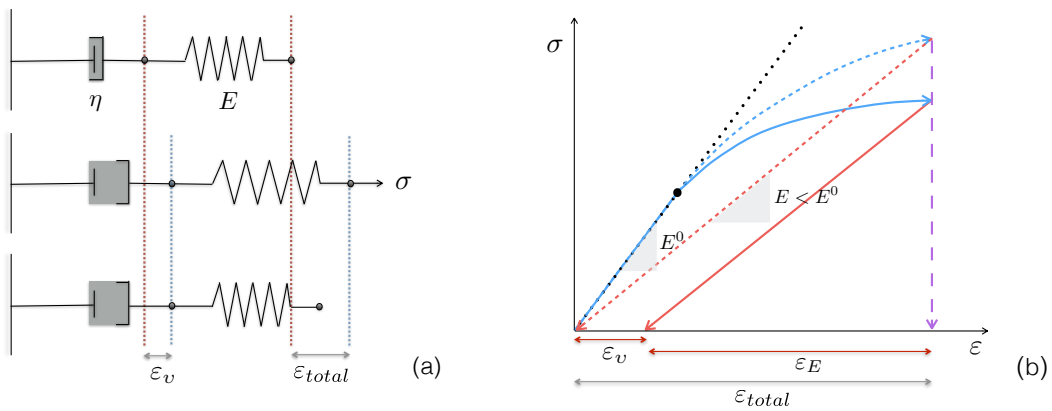
Figure 1. (a) Schematic representations of the Maxwell model for a continuum material with elastic (shear) modulus G E and viscosity η. At time t, a stress is applied on the system. It is removed at time $t + \Delta t$: the spring goes back to its initial position but the dashpot retains its deformation ε_η ε_v. (b) Loading-unloading paths for a material with initial elastic modulus E^0 in the linear-elastic (dotted), EB (dashed) and Maxwell-EB (solid lines) model. The black dot indicates the onset of damaging in the EB and Maxwell-EB models. Unlike the EB model, the Maxwell-EB model allows partitioning the total deformation into a permanent (ε_v) and an elastic contribution (ε_E), as indicated by the ~~red~~ arrows along the deformation axis. The diagram is not to scale in the context of modelling the lithosphere or sea ice : in these geomaterials, permanent deformations can become much greater than elastic deformations as damage events accumulate over time.
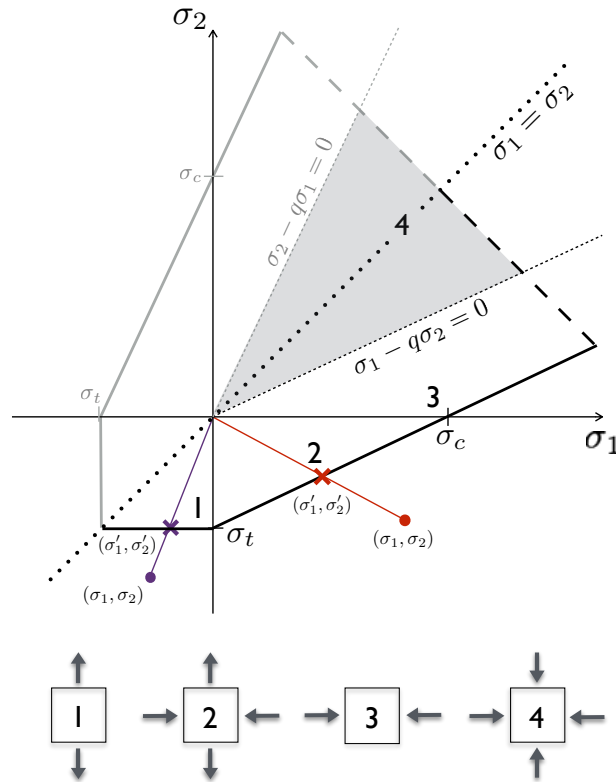
Figure 2. Damage criterion of the Maxwell-EB model in the principal stresses plane (solid line) combining the Mohr-Coulomb and tensile stress criteria. The thick dashed line represents a biaxial compression truncation that closes the envelope but is not applied in the present model. Compression is taken positive and the dotted line indicates the $\sigma_1 = \sigma_2$ axis. Numbers indicate the states of (1) uniaxial tension, (2) biaxial tension and compression, (3) uniaxial compression and (4) biaxial compression and their location relative to the envelope. The calculation of the distance to the damage criterion d_{crit}, defined by the intersection (σ_1', σ_2') of the line relating the state of stress (σ_1, σ_2) of a given element to the origin of the principal stress plane, is represented in red in the case of exceeding the Mohr-Coulomb criterion and in purple, the tensile strength criterion.
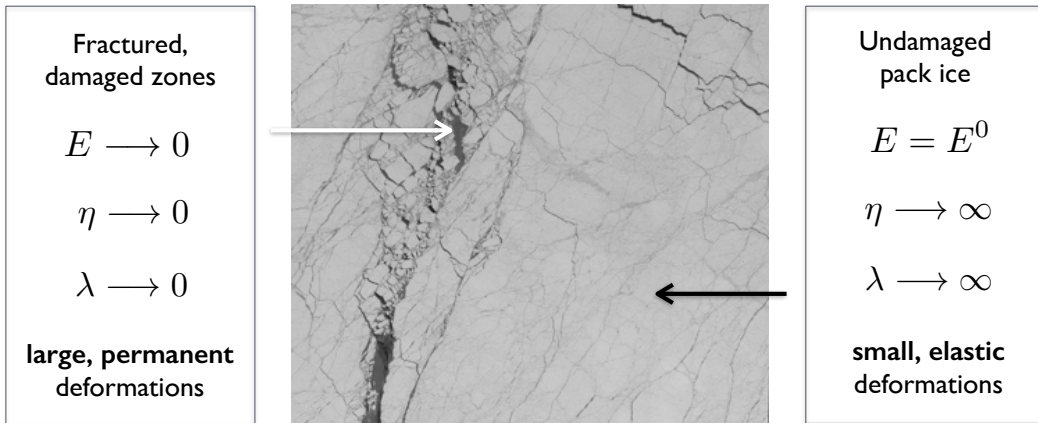
Figure 3. Dependence of the apparent viscosity (η), of the elastic modulus (E) and of the relaxation time (λ) on the level of damage in the Maxwell-EB sea ice model. The image is a SPOT satellite aerial picture of a 59 km $\times$59 km portion of the Arctic sea ice cover centred around 80.18 N, 108.55 W.
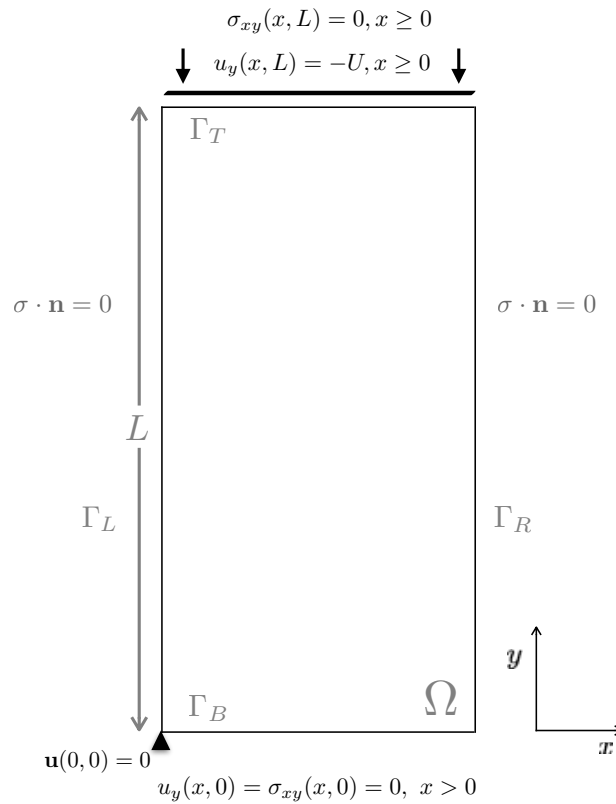

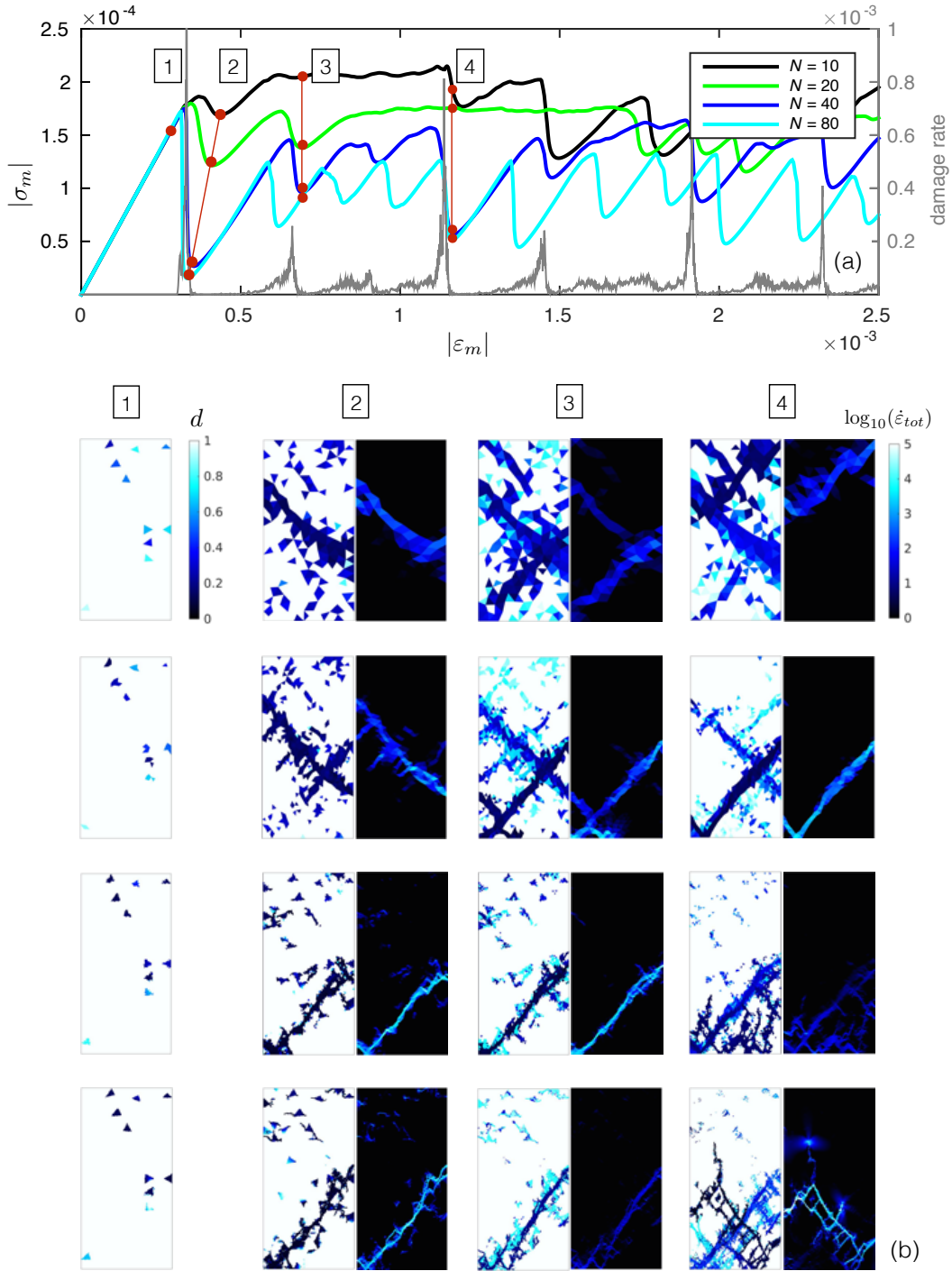**Figure 4.** ~~(a)~~ Domain and boundary conditions for the uniaxial compression experiment.

Figure 5. (a) Macroscopic stress versus macroscopic strain (solid lines) for four uniaxial compression simulations with different spatial resolutions and damage rate (~~dashed~~ number of damaged elements times $1 - d_{crit}$, grey line) for the simulation with $N = 40$. All simulations are initialized with the same values of the mechanical parameters and ~~cohesion~~ with the same field of cohesion (C) defined at the lowest spatial resolution ($N = 10$). (b) Fields of the instantaneous level of damage (left panels) and of the order of magnitude of the total deformation rate ($\log_{10}(\dot{\varepsilon}_{tot})$, right panels) at the four different times indicated on Fig. (a) and for the four simulations (resolution increasing from top to bottom).
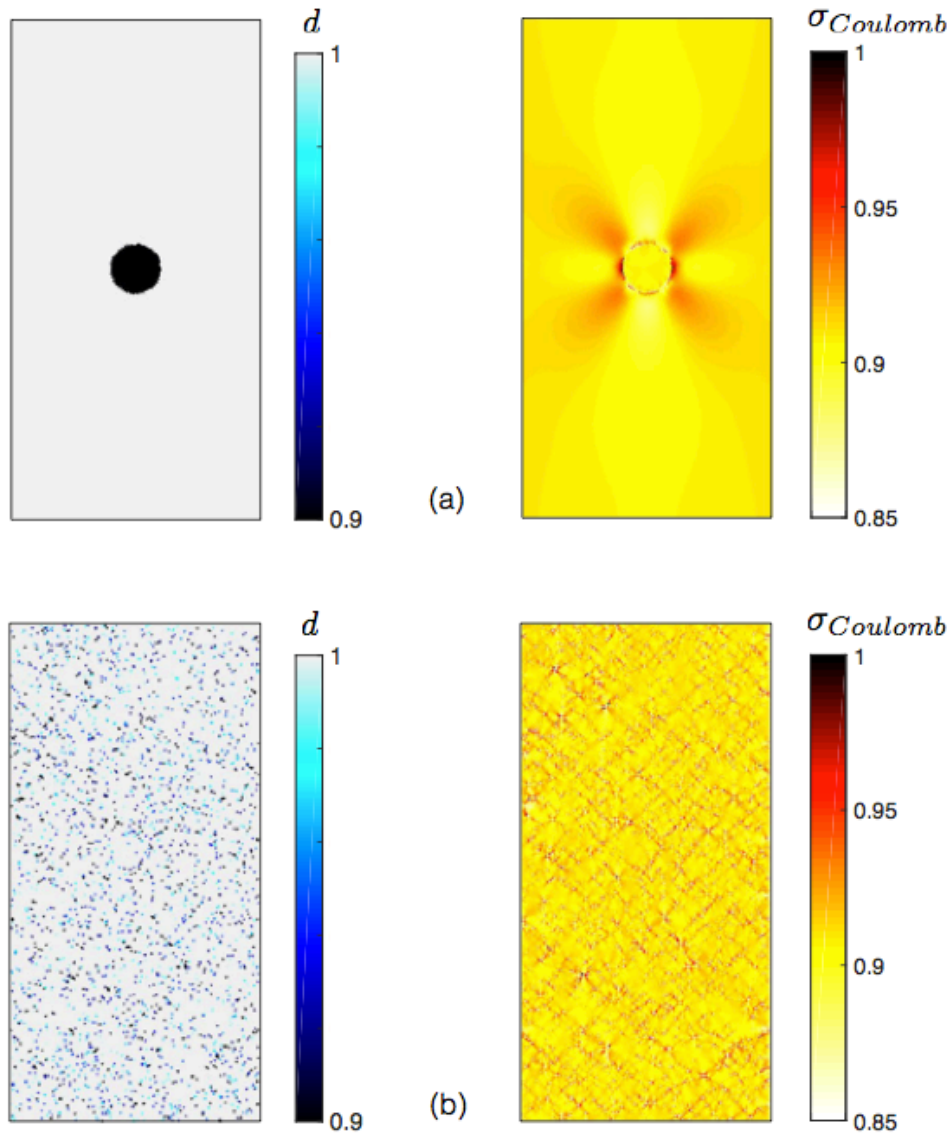
Figure 6. Coulomb's stress field (the normalized maximum stress with respect to the Mohr-Coulomb damage criterion) generated by (a) a circular inclusion defined on the initial field of the level of damage ($d = 0.9$) in an otherwise undamaged ($d = 1$), homogeneous and linear-elastic material (left) and (b) by local damage events within an initially undamaged material in which disorder is introduced through the damage criterion via the field of cohesion, C. In both cases, the plate is subjected to the same uniaxial compression and boundary conditions as described in section 6 and figure 4.
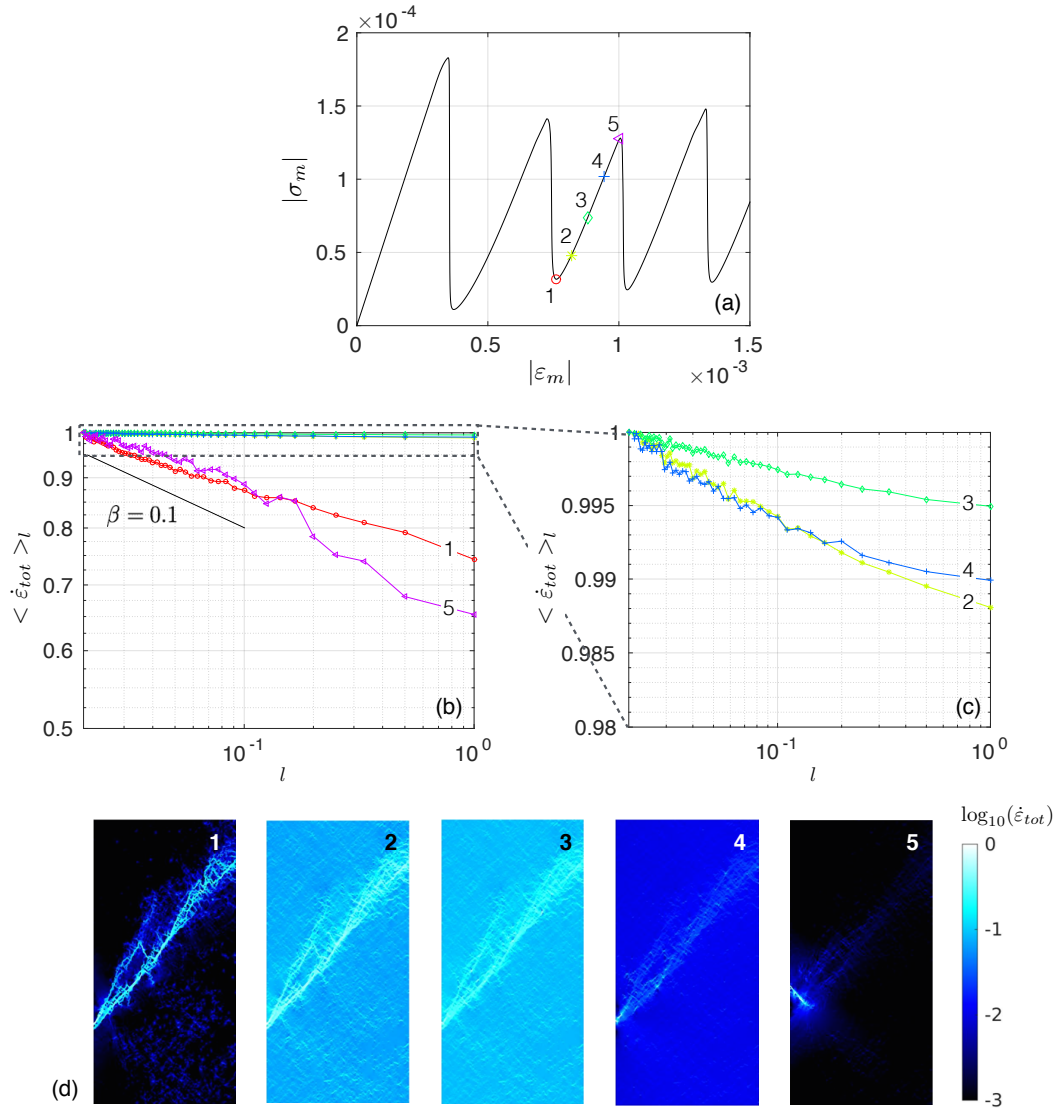
Figure 7. (a) Macroscopic stress as a function of the macroscopic strain for one realization of the uniaxial compression experiment with $N = 100$. (b) Total deformation rate as a function of the spatial scale l ($l = \frac{L}{2n}$ with $1 \leq n \leq N/2$), normalized at the smallest scale L/N, at the five stages indicated on panel (a). (c) Zoom into panel (b) for the second, third and fourth stages. (d) Corresponding fields of the order of magnitude of the total deformation rate ($\log_{10}(\dot{\varepsilon}_{tot})$) normalized by the maximum value of $\dot{\varepsilon}_{tot}$.

41
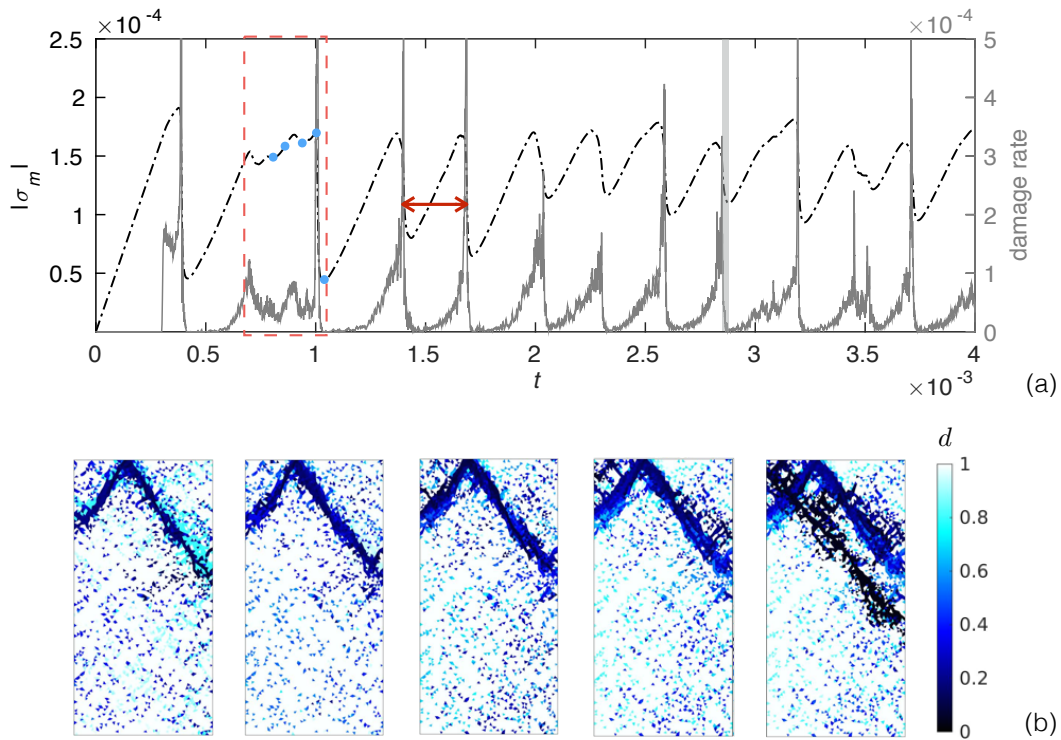
Figure 8. (a) Macroscopic stress (black dashed-dotted line) and damage rate (solid grey line) as a function of time for one realization of the uniaxial compression experiment with $N = 40$. The dashed red box indicates an interval of uninterrupted damaging activity, during which deformation is accommodated by a persisting system of interacting faults. (b) Instantaneous fields of the level of damage at the five times indicated by the blue dots on the macroscopic stress curve, showing the formation of the system of faults (first panel), which remains active for some time (three following panels), until the propagation of a new, non-interacting fault (last panel).
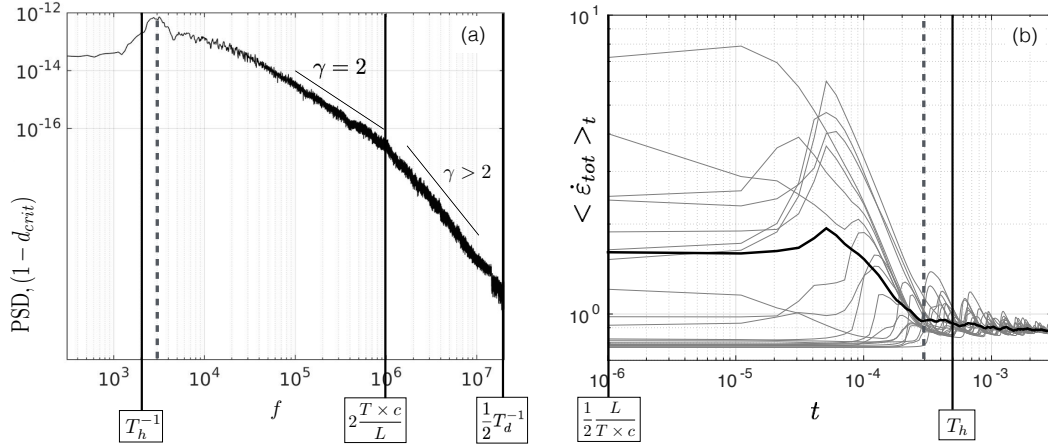
Figure 9. (a) Average power spectral density of the damage rate time series for 5 realizations of the uniaxial compression experiment initialized with different fields of C and with $N = 40$. Vertical solid lines indicate, from left to right, the frequency associated with the characteristic time for healing, the inverse time of propagation of damage across the width of the domain and $\frac{1}{2} \times$ the frequency associated with the characteristic time for damage. The dashed line indicates the frequency of the healing and damaging cycle marked with a red arrow on Fig. 8(a). (b) Total deformation rate $< \dot{\varepsilon}_{tot} >_t$ as a function of the observation time t, for 20 realizations of the coarse graining calculation centred on different arbitrary times t_0 along a uniaxial compression experiment with $N = 40$ (thin grey curves) and average of the 20 realizations (thick black curve). The vertical solid lines indicate, from left to right, the time of propagation of damage across the width of the domain and the characteristic time for healing and the dashed line, the period of the healing and damaging cycle marked with a red arrow on Fig. 8(a).

Parameters		Values
Poisson's ratio	ν	0.3
Internal friction coefficient	μ	0.7
Ice density	ρ	900 kg m^{-3}
Shear wave propagation speed	c	500 ms^{-1}
Undamaged elastic modulus	E^0	$2c^2(1+\nu)\rho \text{ Pa}$
Undamaged apparent viscosity	η^0	$10^7 \times E^0 \text{ Pa s}$
~~Minimum apparent viscosity η_{min} 10^4 Pa s~~ Cohesion	C	$(25-50)\cdot 10^3 \text{ Pa}$
Damage parameter	α	4.0
Undamaged relaxation time	λ^0	$\frac{\eta^0}{E^0} \text{ s}$
Characteristic time for damage evolution	t_d	$\Delta t \text{ s}$
Characteristic time for healing	t_h	10^5 s
Dimensions of compression experiment		**Values**
Length of the ice plate	L	$200 \cdot 10^3 \text{ m}$
Prescribed velocity of forced edge	U	10^{-3} ms^{-1}
Number of elements along short edge	N	10, 20, 40, 80, 100
Mean model resolution	Δx	$\frac{L}{2N} \text{ m}$
Model time step	Δt	$\frac{\Delta x}{c} \text{ s}$
Ice thickness	h	1 m
Ice concentration	A	100%
Variables		**Non-dimensional equivalent**
Horizontal dimension	x	$\tilde{x} = \frac{x}{L}$
Time	t	$\tilde{t} = \frac{tU}{L}$
Ice velocity	$\mathbf{u}$	$\tilde{\mathbf{u}} = \frac{\mathbf{u}}{U}$
Internal stress	σ	$\tilde{\sigma} = \frac{\sigma}{E^0}$ ~~Level of damage d $\tilde{d} = d$ Ice thickness h $\tilde{h} = \frac{h}{H}$~~

Table 1. Model variables, parameters and domain dimensions for the uniaxial compression experiment.